Biogeosciences, 12, 2753–2772, 2015
www.biogeosciences.net/12/2753/2015/
doi:10.5194/bg-12-2753-2015

Biogeosciences Open Access

Sensitivity of the air–sea CO_2 exchange in the Baltic Sea and Danish inner waters to atmospheric short-term variability

A. S. Lansø[1], J. Bendtsen[2], J. H. Christensen[1,3], L. L. Sørensen[1,3], H. Chen[4,5], H. A. J. Meijer[4], and C. Geels[1]

[1]Department of Environmental Science, Aarhus University, 4000 Roskilde, Denmark
[2]Climate Lab, Symbion Science Park, Fruebjergvej 3, 2100 Copenhagen, Denmark
[3]Arctic Research Centre (ARC), Aarhus University, 8000C Aarhus, Denmark
[4]Centre for Isotope Research (CIO), Energy and Sustainability Research Institute Groningen (ESRIG), University of Groningen, Groningen, the Netherlands
[5]Cooperative Institute for Research in Environmental Sciences (CIRES), University of Colorado, Boulder, CO, USA

Correspondence to: A. S. Lansø (asla@envs.au.dk)

Received: 4 September 2014 – Published in Biogeosciences Discuss.: 9 December 2014
Revised: 26 March 2015 – Accepted: 6 April 2015 – Published: 11 May 2015

Abstract. Minimising the uncertainties in estimates of air–sea CO_2 exchange is an important step toward increasing the confidence in assessments of the CO_2 cycle. Using an atmospheric transport model makes it possible to investigate the direct impact of atmospheric parameters on the air–sea CO_2 flux along with its sensitivity to, for example, short-term temporal variability in wind speed, atmospheric mixing height and atmospheric CO_2 concentration. With this study, the importance of high spatiotemporal resolution of atmospheric parameters for the air–sea CO_2 flux is assessed for six sub-basins within the Baltic Sea and Danish inner waters. A new climatology of surface water partial pressure of CO_2 (pCO_2^w) has been developed for this coastal area based on available data from monitoring stations and on-board pCO_2^w measuring systems. Parameterisations depending on wind speed were applied for the transfer velocity to calculate the air–sea CO_2 flux. Two model simulations were conducted – one including short-term variability in atmospheric CO_2 (VAT), and one where it was not included (CAT).

A seasonal cycle in the air–sea CO_2 flux was found for both simulations for all sub-basins with uptake of CO_2 in summer and release of CO_2 to the atmosphere in winter. During the simulated period 2005–2010, the average annual net uptake of atmospheric CO_2 for the Baltic Sea, Danish straits and Kattegat was 287 and 471 Gg C yr^{-1} for the VAT and CAT simulations, respectively. The obtained difference of 184 Gg C yr^{-1} was found to be significant, and thus ignoring short-term variability in atmospheric CO_2 does have a sizeable effect on the air–sea CO_2 exchange. The combination of the atmospheric model and the new pCO_2^w fields has also made it possible to make an estimate of the marine part of the Danish CO_2 budget for the first time. A net annual uptake of 2613 Gg C yr^{-1} was found for the Danish waters.

A large uncertainty is connected to the air–sea CO_2 flux in particular caused by the transfer velocity parameterisation and the applied pCO_2^w climatology. However, as a significant difference of 184 Gg C yr^{-1} is obtained between the VAT and CAT simulations, the present study underlines the importance of including short-term variability in atmospheric CO_2 concentration in future model studies of the air–sea exchange in order to minimise the uncertainty.

1 Introduction

The capacity of ocean and land to take up and re-emit atmospheric CO_2 has a dominating effect on the greenhouse gas balance, and hence changes in climate. Currently, land areas and global oceans are estimated to take up about 27 and 28 %, respectively, of the CO_2 emitted by anthropogenic sources (Le Quéré et al., 2013).

In recent years, biogeochemically active coastal seas have been given increased attention (Borges et al., 2006; Chen et al., 2013; Mørk et al., 2014). Although such coastal waters only amount to 7 % of global oceans, high inputs, production, degradation and export of organic matter might result

in coastal air–sea CO_2 fluxes contributing a great deal more than 7 % to the global air–sea flux (Gattuso et al., 1998). Due to the high heterogeneity of these areas, coastal CO_2 fluxes are prone to large uncertainties. Several studies agree that continental shelves, in general, act as sinks, while estuaries act as sources of CO_2 to the atmosphere. However, global estimates vary in size according to applied methodology, with oceanic uptake in shelf areas between 0.21 and 0.40 $\mathrm{Pg\,C\,yr^{-1}}$, and release from estuaries in the range of 0.10 to 0.50 $\mathrm{Pg\,C\,yr^{-1}}$ (Cai, 2011; Chen et al., 2013; Chen and Borges, 2009; Laruelle et al., 2010). The poor coverage of observations in both space and time makes validation of these global estimates difficult.

In order to better quantify the impact of coastal regions on the global carbon budget, detailed studies of the processes at the regional scale are necessary (Kulinski and Pempkowiak, 2011). A coastal region that has been well studied is the Baltic Sea. The Baltic Sea is a high-latitude inner shelf sea connected to the North Sea through the shallow transition zone of the Danish straits, and enclosed by land with various terrestrial ecosystems and densely populated areas. Seasonal amplitudes of up to 400 µatm are observed in the partial pressure of CO_2 (pCO_2^w) in the Baltic Sea (Thomas and Schneider, 1999) with maximum values of pCO_2^w found in winter and minimum during summer. Since the difference between the pCO_2 level in the ocean and the atmosphere controls the direction of the air–sea CO_2 flux, this is an indication of the pronounced seasonal variation of the flux in the Baltic Sea, with outgassing of CO_2 to the atmosphere during winter and uptake during summer (Thomas et al., 2004; Thomas and Schneider, 1999). Despite numerous studies, it is still uncertain whether the Baltic Sea currently acts as a net sink or source of atmospheric CO_2, as previous studies have given ambiguous results varying from -4.3 to 2.7 $\mathrm{g\,C\,m^{-2}\,yr^{-1}}$ for the entire Baltic Sea region (Gustafsson et al., 2014; Kulinski and Pempkowiak, 2011; Norman et al., 2013). Therefore, it is also difficult to project how the Baltic Sea will contribute to the global carbon budget in the future. Moreover, the region may possibly have changed from being a net source to a net sink of atmospheric CO_2, due to industrialisation and the enormous input of nutrients (Omstedt et al., 2009). These inputs will, however, likely change in the future due to changes in climate and anthropogenic activities (Geels et al., 2012; Langner et al., 2009).

As the Baltic Sea is bordered by land areas, the atmospheric CO_2 concentration found here will be directly affected by continental air leading to greater temporal and spatial variability in the CO_2 level than what is found over open oceans. The impact of temporal variations in atmospheric CO_2 on the air–sea CO_2 exchange has been discussed by Rutgersson et al. (2008) and (2009). They show an overestimation in the amplitude of the seasonal cycle for calculated air–sea CO_2 fluxes, when using a constant annual mean value of atmospheric CO_2 concentration instead of daily levels of atmospheric concentration. Annually, the difference was less than 10 % between the two cases, but weekly flux deviations of 20 % were obtained. This indicates how synoptic variability in the atmosphere cannot always be ignored (Rutgersson et al., 2009). Further, Rutgersson et al. (2008) note that the uncertainties connected with the transfer velocity are much greater than uncertainties related to temporal variations in atmospheric CO_2. However, it is still worthwhile to minimise the bias in the estimation of the flux by including detailed information on atmospheric CO_2 concentrations. The short-term variability (hourly) of both meteorology and atmospheric CO_2 concentrations is not always accounted for or has not been discussed in previous estimates of the air–sea CO_2 fluxes in the Baltic Sea (Algesten et al., 2006; Gustafsson et al., 2014; Kulinski and Pempkowiak, 2011; Löffler et al., 2012; Norman et al., 2013; Wesslander et al., 2010) .

The present study aims to determine the importance of the short-term variability in atmospheric CO_2 concentrations on the net air–sea CO_2 flux of the Baltic Sea and Danish inner waters (which consists of Kattegat and the Danish straits; Øresund and the Belt Seas). A modelling approach is applied, which includes both short-term (hourly to synoptic) and long-term (seasonal to interannual) variability in the atmospheric CO_2 concentrations. The analysis is carried out by constructing a mesoscale model framework based on an atmospheric transport model covering the study region in high resolution in both space and time. The model includes a new spatial pCO_2^w climatology developed especially for the investigated marine area, as existing climatologies do not cover this area. The advantages of the present study are that the same and consistent method is applied to the entire Baltic Sea and Danish inner waters, and that the impact of spatial and temporal short-term variability in atmospheric parameters will be investigated in more detail than in the previous studies of this region.

Recently, national CO_2 budgets that include both anthropogenic and natural components have been estimated for various countries (Meesters et al., 2012; Smallman et al., 2014). The present study is likewise part of a national project, Ecosystem Surface Exchange of Greenhouse Gases in an Environment of Changing Anthropogenic and Climate forcing (ECOCLIM), which is determining the CO_2 budget for Denmark. For that reason, the present study will also estimate the marine component of the Danish CO_2 budget.

In Sect. 2 the study area, the applied surface fields of pCO_2^w and the model framework are described. Results are presented in Sect. 3, leading to a discussion in Sect. 4 and with concluding remarks in Sect. 5.

2 Study setup

2.1 Study area

The marine areas investigated in this study are shown in Fig. 1. In the following, a short introduction to these hetero-

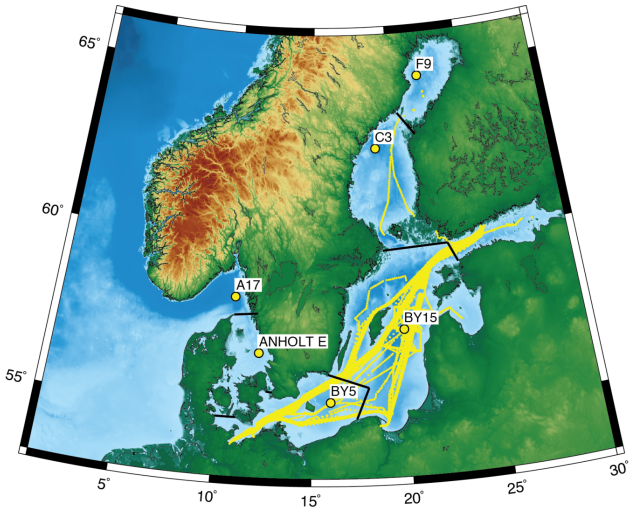

Figure 1. The locations of the six monitoring stations in the Baltic Sea, where surface pCO_2^w values are calculated (SHARK database, 2013). The stations are located in Skagerrak (A17), Kattegat and the Danish straits (Anholt E), the western Baltic Sea (BY5), Baltic proper (BY15), the Bothnian Sea (C3) and the Bay of Bothnia (F9). Data from on-board measurements of surface pCO_2^w are shown in yellow and cover, in particular, the area between Kiel and Helsinki. The division of the six sub-domains is indicated with black lines.

geneous marine areas is given as well as a description of the overall atmospheric CO_2 field in the region.

The Baltic Sea is a semi-enclosed continental shelf sea area with a large volume of river runoff adding a substantial amount of nutrients and terrestrial carbon to the Baltic Sea (Kulinski and Pempkowiak, 2011). The circulation in the Baltic Sea is influenced by a relatively large runoff from the surrounding drainage areas, and this causes a low-salinity outflowing surface water mass from the area. The Baltic Sea can, therefore, be considered a large estuary. Inflow of high-salinity water from the North Sea ventilates the bottom waters of the Baltic Sea, and the exchange between these water masses occurs through the shallow North Sea/Baltic Sea transition zone centred around the Danish straits (Bendtsen et al., 2009). Ice coverage is observed in the northern part of Baltic Sea during winter (Löffler et al., 2012), which has implications for the air–sea exchange of CO_2. The ice extent in the Baltic Sea during 2005–2010 fluctuated between average conditions in the winter 2005–2006 (ice cover of 210 000 km^2), a general mild period in the winters between 2007–2009 (with a minimum ice cover of 49 000 km^2 in 2007–2008) and a severe winter condition in 2010–2011 where the sea ice extent reached a maximum value of 309 000 km^2 (Vainio et al., 2011). Thus, there was no apparent trend of the sea ice extent in the simulation period.

Atmospheric concentrations of CO_2 in the Baltic region have a greater seasonal amplitude than at, for example, Mauna Loa, Hawaii, which often is referred to as a global reference for the atmospheric CO_2 background, due to the remoteness of the site. The larger seasonal amplitude over the Baltic can be explained by the difference in latitude between the studied area (54–66° N) and Mauna Loa (20° N), and the undisturbed air at the high altitude site of Mauna Loa compared to the semi-enclosed Baltic Sea (Rutgersson et al., 2009). The study by Rutgersson et al. also showed that the atmospheric CO_2 concentration in the southern part of the Baltic Sea is more affected by regional anthropogenic and terrestrial sources and sinks than the more remote northern part of the Baltic Sea area.

2.2 Surface water pCO_2^w climatology

Model calculations of the surface air–sea gas exchange of CO_2 are parameterised in terms of the difference in partial pressure of CO_2 (i.e. ΔpCO_2) between the atmosphere and the ocean surface. The global climatology of oceanic surface pCO_2^w by Takahashi et al. (2009) is commonly used in atmospheric transport models of CO_2 (e.g. Geels et al., 2007; Sarrat et al., 2009) and is also applied here for areas outside the Baltic Sea and Danish inner waters. However, this climatology does not cover the Baltic Sea area, and therefore, a new Baltic Sea climatology has been created and merged with the climatology of Takahashi et al. (2009) in the model domain towards the North Sea and the northern North Atlantic.

Available pCO_2^w surface measurements and water chemistry data from the Baltic Sea and Danish inner waters are combined in six sub-domains of the Baltic Sea to provide monthly averaged pCO_2^w values for this new climatology. The sub-domains cover Skagerrak, Kattegat and the Belt Sea (henceforth referred to just as Kattegat), the western Baltic Sea, the Baltic proper, the Gulf of Finland, the Bothnian Sea and the Bay of Bothnia. Two data sets are analysed: one from marine stations (stationary) and the other obtained from ships (on-board). All available data collected since the year 2000 is included in the analysis (Fig. 1). Hence, measurements from a depth of 5 m from all stations were averaged for the period 2000–2012, and on-board pCO_2^w measurements from the surface layer (surface intake approximately 5 m) were averaged for the period 2000–2011. From the two data sets monthly mean values for each sub-domain are determined.

Surface measurements of salinity, temperature, alkalinity and pH from six marine measuring stations (operated by the Swedish Meteorological and Hydrological Institute, SMHI; SHARK database, 2013) are applied to calculate the surface pCO_2^w values by a similar approach as described in Wesslander et al. (2010). The six stations are located from the central Skagerrak to the Bay of Bothnia (Fig. 1), but no measurements are available from the Gulf of Finland. A relatively high frequency of observations is obtained at the six monitoring stations with the number of observations in each month ranging between 4–8 at station A17, 15–36 at station Anholt E, 6–18 at station BY5, 7–17 at station BY15, 1–5 at station C3 (but no data representing November) and 2–10 at station

F9 (but no data representing January, February and November).

Surface levels of pCO_2^w from the central Baltic Sea (Schneider and Sadkowiak, 2012) have been measured by on-board pCO_2^w systems (Körtzinger et al., 1996; Schneider et al., 2006) from cargo and research ships. In particular, a route between Germany (Kiel) and Finland (Helsinki) has regularly been monitored from cargo ships, whereas no measurements are available in the northern part of the Baltic Sea, the Danish straits, Kattegat and Skagerrak. Good data coverage of on-board pCO_2^w measurements is obtained in the sub-domain of the western Baltic Sea, with the number of observations in each month ranging between 9000 and 55 000, and in the Baltic proper, where the corresponding number of observations ranges from 20 000 to 116 000. In the Bothnian Sea the number of observations ranges from 2000 to 77 000, but there are no observations in December. Only a single month (March) is represented in the Bay of Bothnia with about 5000 observations. The Gulf of Finland is represented with observations ranging from 3000 to 18 000 each month.

The stationary data from the monitoring stations and the on-board data have been combined in such a manner that if on-board data exists for a sub-domain, these data is used for the pCO_2^w fields in the given subdomain. Otherwise, measurements from the monitoring stations are used to calculate the pCO_2^w fields. Thus, pCO_2^w fields for Skagerrak, Kattegat, and the Bay of Bothnia are calculated solely based on data from the SMHI stations. The pCO_2^w fields for the western Baltic Sea, the Baltic proper, the Gulf of Finland and the Bothnian Sea are obtained from the on-board measurements of pCO_2^w, except for December in the Bothnian Sea, which is represented by the monitoring station C3. The data used to obtain the monthly averages of surface pCO_2^w in each subdomain have all been normalised to the year 2000 using an annual increase in CO_2 of 1.9 µatm yr^{-1} found for the central Baltic Sea (Wesslander et al., 2010).

The resulting pCO_2^w climatology for the Baltic Sea and Danish inner waters is combined with the global open ocean pCO_2^w climatology from Takahashi et al. (2009). This climatology is calculated for a global oceanic grid with a horizontal resolution of $5^\circ \times 4^\circ$ in longitude and latitude, respectively. Consequently, this field has an even coarser spatial resolution than the sub-domains defined in the Baltic Sea area. The global climatology is by Takahashi and colleagues, referenced to the year 2000 with an annual trend of 1.5 µatm yr^{-1}. This trend is also used to extrapolate the global data for the year 2000 to the proceeding years covered in this study. Note that the trend used for the Baltic Sea and Danish inner waters is 1.9 µatm yr^{-1}, as this trend is shown to match this particular area. However, the difference in annual trends between the two climatologies is so small compared to the absolute pCO_2^w values, and thus it is reasonable to assume that the impact on the current results will be insignificant.

The monthly averaged pCO_2^w values show a characteristic seasonal pattern at all monitoring stations and for the on-board pCO_2^w data (Fig. 2, and Table S1 and Fig. S1 in the Supplement). The surface pCO_2^w is under-saturated during spring and summer and super-saturated during autumn and winter (Fig. 3a). However, there is a large spatial gradient in the seasonal amplitude from Skagerrak to the Baltic Sea. A seasonal amplitude of about 140 µatm characterises the variation in Skagerrak and Kattegat, where the pCO_2^w varies between 275 and 420 µatm, and the surface water is only slightly super-saturated during the winter months. In the Baltic Sea, a relatively large seasonal amplitude of up to 400 µatm is observed, as primary production during the growing season, i.e. spring and summer, causes a large uptake of total dissolved inorganic carbon in the surface layer and contributes to lowering the surface pCO_2^w values. The data shows how biological uptake causes a reduction of surface pCO_2^w, despite the general warming during the summer months, which normally tends to increase the pCO_2^w in the surface water. During autumn and winter, the surface pCO_2^w values increase because sub-surface waters enriched in total dissolved inorganic carbon from remineralisation of organic matter during the summer are mixed into the surface layer. In the areas north-east of the western Baltic Sea, in particular, this allows for high monthly averaged surface pCO_2^w values of 460–530 µatm during winter with the largest average winter values observed in the Gulf of Finland.

The calculated pCO_2^w values at the monitoring stations agree well the on-board pCO_2^w data. The on-board pCO_2^w data includes both temporal and spatial variability within each sub-domain during the period since 2000. Therefore, their standard deviations (SD) are larger than the SDs from the monitoring stations, which mainly arise due to interannual variability in the period. Two sub-domains, the western Baltic Sea and the Baltic proper, have good data coverage from both the monitoring stations and on-board pCO_2^w data. The stations, BY5 and BY15, that represent the western Baltic Sea and the Baltic proper, respectively, have lower surface pCO_2^w values during the summer period than the on-board pCO_2^w data, but the difference between the two data sets are within their SD.

2.3 Model framework

The model framework is based upon the Danish Eulerian Hemispheric Model (DEHM) – a well validated three-dimensional large-scale atmospheric chemical transport model (Brandt et al., 2012; Christensen, 1997). DEHM is based on the equation of continuity and uses terrain following sigma levels as vertical coordinates. Here, 29 vertical levels are distributed between the surface and 100 hPa with a higher density of vertical levels in the lower part of the atmosphere. The main domain of DEHM covers the Northern Hemisphere with a horizontal grid resolution of 150 km × 150 km using a polar stereographic projection

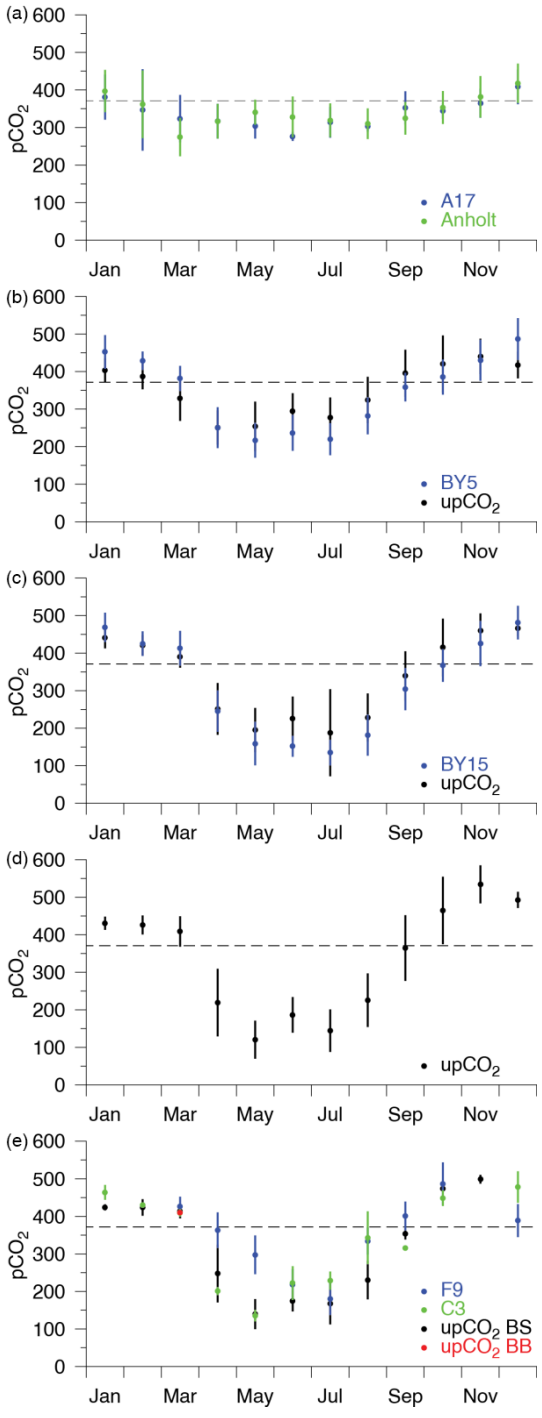

Figure 2. Monthly averaged surface pCO_2^w values from the six monitoring stations and from on-board pCO_2^w data in the sub-domains in the study region. Monthly averaged values are shown with bullets together with the standard deviations. **(a)** Values from monitoring stations in Skagerrak (A17, blue) and Kattegat (Anholt E, green), **(b)** station BY5 (blue) and on-board pCO_2^w in the western Baltic Sea (black), **(c)** station BY15 (blue) and on-board pCO_2^w from the Baltic proper (black), **(d)** on-board pCO_2^w data from the Gulf of Finland and **(e)** station F9 (blue), C3 (green) and on-board pCO_2^w data from the Bothnian Sea (black) and on-board pCO_2^w from March in the Bay of Bothnia (red).

true at 60° N. Furthermore, DEHM has nesting capabilities allowing for a nest over Europe with a resolution of 50 km × 50 km, a nest of northern Europe with an approximate resolution of 16.7 km × 16.7 km, and a 5.6 km × 5.6 km nest covering Denmark. In order to cover the Baltic Sea and Danish marine areas in focus, a setup with two nests is applied in the current study (the European and the northern European nests). The main domain and the nests each comprise of 96 × 96 grid points. This study uses a modified version of DEHM solely simulating transport and exchange of CO_2 (Geels et al., 2002, 2004, 2007), but with an updated description of the surface exchange of CO_2 (described in Sect. 2.2.1). DEHM is driven by meteorological data from the meteorological model MM5v3.7 (Grell et al., 1995) using National Centers for Environmental Prediction, NCEP, data as input.

2.3.1 Model inputs

To accurately simulate the atmospheric content of CO_2, a number of CO_2 sources and sinks within the model domain as well as inflow at the lateral boundaries are required together with a background concentration. The atmospheric concentration of CO_2 (X_{atm}) can be described by

$$X_{atm} = X_{ff} + X_{bio} + X_{fire} + X_{ocn} + X_{background}, \quad (1)$$

where X_{ff} is the contribution of CO_2 from fossil fuel emissions, X_{fire} from vegetation fires and X_{bio} and X_{ocn} are the contribution to the atmospheric concentration from exchange of CO_2 with the terrestrial biosphere and ocean, respectively. $X_{background}$ is the atmospheric background of CO_2.

Fossil fuel (X_{ff})

Fossil fuel emissions for the domain covering the Northern Hemisphere are implemented in DEHM from the CarbonTracker (hereafter referred to as CT) simulation system (CarbonTracker CT2011_oi, 2013; Peters et al., 2007). This emission map has a 3-hourly temporal resolution on a 1° × 1° grid.

For the European area, the CT values are replaced by a fossil fuel emission inventory with a higher spatiotemporal resolution (hourly, 10 km × 10 km) developed by the Institute of Energy Economics and the Rational Use of Energy (Pregger et al., 2007).

For the area of Denmark, emissions with an even finer spatial resolution of 1 km × 1 km are applied obtained from the Department of Environmental Science, Aarhus University. These are based on the Danish national inventory submitted yearly to UNFCCC (United Nations Framework Convention on Climate Change) and constructed from energy statistics, point source and statistic sub-models (Plejdrup and Gyldenkærne, 2011).

As the European and Danish emission inventories are for the years 2005 and 2011, respectively, these inventories are

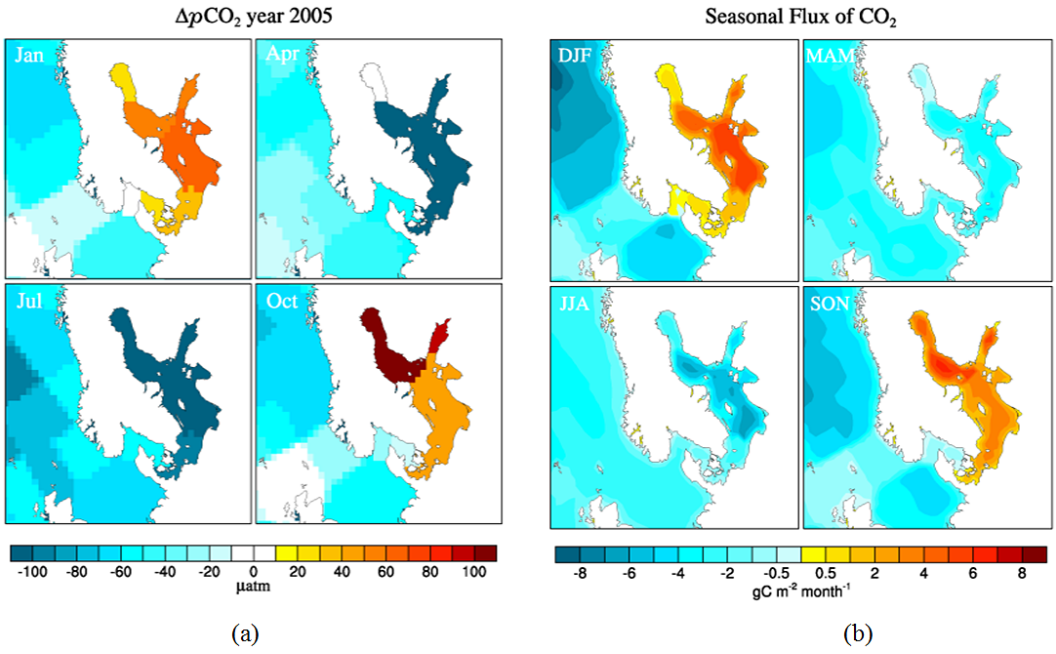

Figure 3. (a) ΔpCO_2 for selected months during 2005. For the calculations of ΔpCO_2, the combined surface map of the global pCO_2^w climatology by Takahashi et al. (2009) and the climatology for the Baltic Sea constructed in this study are used. The coarse resolution of the global climatology is clearly visible along the west coast of Norway. Periods of under and over-saturation are seen which indicate the direction of the air–sea CO_2 flux (positive ΔpCO_2 indicates release of CO_2 to atmosphere, negative values indicate uptake). **(b)** The mean seasonal air–sea CO_2 flux for the years 2005 to 2010 in g C m^{-2} month^{-1} for the VAT simulation. Positive sign indicates release of CO_2 from the ocean to the atmosphere, negative sign indicates uptake of atmospheric CO_2 by the ocean. This sign convention is used throughout the paper.

scaled to total yearly national estimates of carbon emissions from fossil fuel consumption conducted by the Carbon Dioxide Information Analysis Center, CDIAC, in order to account for the year-to-year change in emissions (Boden et al., 2013).

Biosphere (X_{bio})

Terrestrial biosphere fluxes from the CT system, with a spatial resolution of $1° \times 1°$ and a temporal resolution of 3 h, are applied in DEHM. In the CT assimilation system, the Carnegie–Ames–Stanford Approach (CASA) biogeochemical model is used for prior fluxes (Giglio et al., 2006; van der Werf et al., 2006). The prior terrestrial biosphere fluxes are optimised in the CT assimilation system by atmospheric observations of CO_2. Via this atmospheric inversion a best guess of surface fluxes is obtained, and the optimised fluxes are implemented in DEHM.

Fires (X_{fire})

CO_2 emissions due to vegetation fires are obtained from the CT fire module and applied in DEHM. The CT fire module is based on the Global Fire Emission Database, GFEDv3.1, and CASA, while the burned area from GFED is based on MODIS satellite observations of fire counts. The resolution is likewise 3-hourly on a $1° \times 1°$ grid.

Ocean (X_{ocn})

The CO_2 flux (F) at the air–sea interface is calculated using the relationship: $F = k\alpha\Delta pCO_2$, where, k is the exchange coefficient, α is the gas solubility and ΔpCO_2 is the difference in partial pressure of CO_2 between the surface water and the overlying air. The gas solubility of CO_2 is determined from Weiss (1974) and depends on the water temperature and salinity. A $0.25° \times 0.25°$ salinity map is implemented in DEHM for the calculation of CO_2 solubility (Boyer et al., 2005). To calculate ΔpCO_2, the surface pCO_2^w fields described in Sect. 2.2 are applied together with the concentration of CO_2 in the lowest atmospheric layer in DEHM.

No standardised parameterisation of the transfer velocity, k, exists, but k is most often parameterised as a power function of the wind speed (Garbe et al., 2014; Rutgersson et al., 2008) normalised to the Schmidt number (Sc) according to Wanninkhof (1992). In the present study we use the parameterisation of Wanninkhof (1992; hereafter referred to as W92). This parameterisation has been used in many previous studies within the study area (Löffler et al., 2012; Rutgersson et al., 2008; Wesslander er al., 2010), and by using W92 this allows for a direct comparison of the estimated fluxes. W92 is a function of the wind speed at 10 m above the surface (u_{10}) and when normalised to Sc at 20 °C in salt water it takes the

form

$$k_{660} = \left(0.31u_{10}^2\right)\sqrt{\frac{660}{Sc}}. \quad (2)$$

However, a few additional parameterisations that could be more representative of the study area are also tested. One is from Nightingale et al. (2000), who estimate a transfer velocity based on tracer gas measurements in the North Sea of

$$k_{660} = \left(0.333u_{10} + 0.222u_{10}^2\right)\sqrt{\frac{660}{Sc}}. \quad (3)$$

Another is by Weiss et al. (2007), who carried out measurements using eddy covariance techniques in the Arkona basin located within the Baltic Sea to estimate an accurate k for this particular area. This parameterisation takes the form

$$k_{660} = \left(0.365u_{10}^2 + 0.46u_{10}\right)\sqrt{\frac{660}{Sc}}. \quad (4)$$

The parameterisation by Weiss et al. (2007) often yields greater values than other transfer velocity parameterisations; however, it will be applied here, as the experiment was conducted within the study area.

Sea ice coverage is in DEHM obtained from NCEP. The sea ice coverage is implemented in the calculations of the air–sea CO_2 exchange, such that the flux in a grid cell is reduced by the fraction of sea ice. If the fraction of sea ice coverage is 1, the entire grid cell will be covered with ice, and no exchange of CO_2 will take place between the ocean and atmosphere. Recent studies have shown that CO_2 exchange between ice-covered sea and the atmosphere does take place, but to what extent has not yet been quantified (Parmentier et al., 2013; Sørensen et al., 2014). For that reason, the exchange over sea ice is not accounted for here.

k_{660}, α and ΔpCO_2 are calculated at each time step of the model simulation (the time step of the model varies between ca. 3 and 20 min depending on, for example, the nest). Consequently, the air–sea CO_2 flux has the same temporal resolution as the simulated atmospheric CO_2.

Atmospheric background ($X_{\text{background}}$)

The level of atmospheric CO_2 has been increasing since pre-industrial times. It is not feasible to simulate this entire time period with the model system to replicate this build-up. Therefore, an atmospheric background of CO_2 is needed. The atmospheric background of CO_2 is established on the basis of the NOAA ESRL GLOBALVIEW-CO2 data product using observations from the Baltic station, BAL (55°35′ N, 17°22′ E; GLOBALVIEW-CO2, 2013). BAL lies within the area of interest, but far from local sources and sinks. It can, therefore, be assumed to represent the atmospheric background level in the study area. The atmospheric background of CO_2 is calculated based on the following equation:

$$X_{\text{background}} = X_{\text{CO}_2\,2000} + 1.91(\text{year} - 2000) + 0.16\,\text{month}. \quad (5)$$

Here, $X_{\text{CO}_2\,2000} = 370.15$ ppm is the mean CO_2 concentration at the station in 2000, year and month is the simulated year and month, and 1.91 and 0.16 represent the yearly and monthly trend of atmospheric CO_2. The trends are based on the times series at BAL for the period 2000–2010, in order to get a representative overall trend for the period in focus here (2005–2010).

Boundary conditions

DEHM only covers the Northern Hemisphere; hence, boundary conditions for the main domain are needed at the lateral boundaries towards the Southern Hemisphere to account for inflow from the Southern Hemisphere. Three-dimensional atmospheric mole fractions of CO_2 from the CT system are applied at these boundaries.

3 Results

3.1 Model evaluation

The period 2005–2010 is simulated by DEHM with setup and fluxes as described in Sect. 2. The performance of the model for this period is evaluated by comparing simulated atmospheric CO_2 concentrations against observed. The comparison is made at six stations within the study area where both remote continental (PAL), marine (F3, MHD, OST, WES) and anthropogenic (LUT) influenced stations are represented.

Measured and simulated atmospheric CO_2 from the marine site Östergarnsholm, Sweden (OST, 57°27′ N, 18°59′ E) and the anthropogenic continental site Lutjewad, the Netherlands (LUT, 53°40′ N, 6°31′ E; van der Laan et al., 2009) are shown for the year 2007 in Fig. 4. The Östergarnsholm marine micrometeorological field station has been running semi-continuously since 1995, measuring atmospheric CO_2 since 2005. The site has been shown to represent marine conditions and is described further in Rutgersson et al. (2008) and Högström et al. (2008). Hourly mean concentrations are plotted for simulated and measured atmospheric CO_2, and at both sites a large diurnal variability is seen in the observations. The model is not able to capture the large amplitude in the diurnal cycle, but correlations of 0.75 and 0.71 are obtained for LUT and OST, respectively. The root mean square errors, RMSE, are 9.6 and 8.8 ppm, respectively. These high RMSEs are linked to the underestimation of the diurnal cycle in the model. Earlier model studies have shown the same tendency to underestimate the observed variability (e.g. Geels et al., 2007). The underestimation of the diurnal cycle by DEHM is most likely caused by the coarse spatial resolution of the biosphere fluxes. Further, weekly averages are made for both observed and modelled concentrations of atmospheric CO_2 (see Fig. 4). Improvements are obtained in

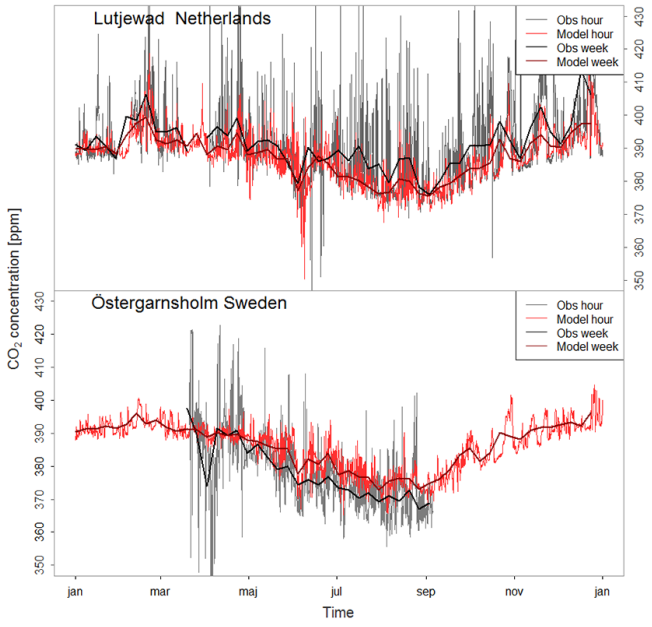

Figure 4. One-hour averages of modelled and continuously measured atmospheric CO_2 concentrations in 2007. Also, weekly averages of both modelled and measured CO_2 concentrations are shown.

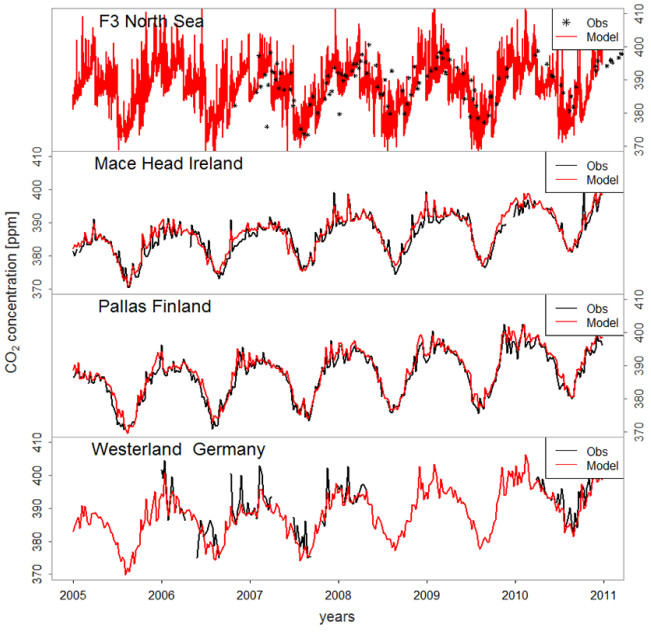

Figure 5. The top panel shows hourly averages of modelled atmospheric CO_2 concentrations compared to flask measurements at F3. The three panels below include comparisons of weekly averages of modelled and continuous measurements of CO_2 at MHD, PAL and WES for the period 2005–2010.

both correlation and RMSE to 0.89 and 5.3 ppm for LUT, and 0.91 and 5.6 ppm for OST. Synoptic-scale variability is seen in the atmospheric CO_2 concentration in both the simulated and observed time series. In particular, at LUT, large positive spikes are seen due to the influence of air from densely populated and industrialised regions.

Flask measurements of CO_2 at F3, an oil and gas platform in the Dutch exclusive economic zone of the North Sea approximately 200 km north of the Dutch coast (54°51′ N, 4°44′ E; van der Laan-Luijkx et al., 2010) are compared to hourly modelled averages (Fig. 5) during the 6-year simulated period. This results in a correlation of 0.64 and an RMSE of 5.7 ppm. Local sources can influence the measured CO_2 concentration under certain wind conditions at F3. Consequently, the most extreme outliers were filtered out with the help of simultaneous CH_4 and CO measurements, when the influence from the local source was obvious. Continuous measurements at F3 conducted in a previous study (van der Laan-Luijkx et al., 2010) and covering a shorter period have indicated that the diurnal variation in the CO_2 concentration at this marine site F3 is negligible. Day-to-day variations related to synoptic changes in the wind direction etc. is according to van der Laan-Luijkx et al. seen in the continuous data. This pattern is captured by the DEHM model. Thus, the underestimation of the diurnal cycle by DEHM over land (as seen at LUT and OST), might only affect the current study at the near-coastal areas, whereas CO_2 concentrations simulated by DEHM over open waters are more representable.

To examine the model performance on a longer timescale, weekly averages are made for the two marine stations Mace Head, Ireland (MHD, 53°20′ N, 9°54′ W; Biraud et al., 2000) and Westerland, Germany (WES, 54°56′ N, 8°19′ E; UBA, 2014) and the remote continental station, Pallas-Sammaltunturi, Finland (PAL, 67°58′ N, 24°07′ E; FMI, 2013) for the 6-year period (Fig. 5). In general, a reasonable correspondence between model and observations is seen during this period with correlations of 0.96, 0.98 and 0.89, and RMSEs of 1.8, 1.9 and 3.8 ppm for MHD, PAL and WES, respectively. The ability of the model to capture the seasonal cycle contributes to the very high correlation, but the model is also capable of capturing weekly variability and transport events especially during winter.

To conclude, this evaluation shows that the DEHM model captures the overall atmospheric CO_2 pattern across the marine region in focus in the current study.

3.2 Air–sea CO_2 fluxes

In order to investigate the effect of short variability in atmospheric CO_2 concentrations on the air–sea CO_2 flux, two different model simulations are conducted. One model simulation has atmospheric CO_2 concentrations that vary from time step to time step according to the fluxes and atmospheric transport in DEHM. This is in the following referred to as the VAT ("Variable ATmosphere") simulation. The other simulation contains at each time step and grid cell the monthly mean

CO_2 concentration for the given month. This is in the following referred to as CAT ("Constant ATmosphere"). All other settings are identical in the two simulations. The simulations are made for the period 2005 to 2010 using the transfer velocity parameterisation by W92.

First, the results of atmospheric CO_2 concentrations and air–sea CO_2 fluxes from the VAT simulation will be presented. These results can be used to get an understanding of how the atmospheric CO_2 concentrations vary, and of how the air–sea CO_2 fluxes behave in terms of size and direction in the different sub-basins of the Baltic Sea and Danish inner waters. This will be followed by the comparison of the VAT and CAT simulation.

3.2.1 Variable atmospheric CO_2 concentration

The variability of atmospheric CO_2 in the Baltic area is illustrated in Fig. 6, which shows a few examples of the hourly simulated surface concentration. The top panels show the variability in February 2007, where synoptic-scale variability influence transport of CO_2, and hence the surface concentrations. On 1 February 2007 at 04:00 GMT, a low pressure system had during the past few days moved through southern Scandinavia and was then located over Poland. This system has rotated continental air with high levels of CO_2 from the east towards the Baltic Sea. On 3 February 2007, the prevailing winds were then westerly, where marine air masses with lower CO_2 concentrations were transported towards the Baltic Sea. The lower panels of Fig. 6 show the diurnal variability on 14 July 2007. At 02:00 GMT, air masses with high CO_2 concentrations were transported from land towards the marine areas – most evident in near-coastal areas. The same is the case at 14:00 GMT, but with lower concentrations due to extensive atmospheric mixing (a deep atmospheric boundary layer) and the uptake of CO_2 by the terrestrial biosphere at this time of the day. These examples show that large spatial gradients of up to 20 ppm can develop across the Baltic Sea during summer.

The seasonal averaged air–sea CO_2 fluxes estimated by DEHM in the VAT simulation are shown in Fig. 3b. In winter, a gradient is seen from the North Sea through the Danish inner straits towards the Baltic Sea, indicating a large release of CO_2 to the atmosphere in the Baltic, and uptake in the North Sea. Progressing to spring, the gradient towards the Baltic ceases and all areas now have marine uptake of atmospheric CO_2, which continues throughout the summer. In autumn, the gradient starts to build up again, and the Baltic Sea becomes a source of CO_2 to the atmosphere.

The monthly mean 2005–2010 sub-basin averaged fluxes likewise depict this seasonality (Fig. 7). The highest seasonal amplitudes are found in the Baltic Sea area stretching from the Baltic proper and northwards with the greatest seasonal amplitude of 12 g C m^{-2} $month^{-1}$ found in the Bothnian Sea. Less seasonal variation in the CO_2 flux is obtained for Kattegat and the Danish straits, which experience a yearly variability of just 4.3 g C m^{-2} $month^{-1}$.

The total sub-basin monthly mean fluxes of CO_2 between the atmosphere and ocean show a seasonal variation for all areas with release in winter and uptake of atmospheric CO_2 in summer (Table 1). The entire area comprising of the six sub-basins has for the period 2005–2010 an average annual net uptake of atmospheric CO_2 of 287 Gg C yr^{-1}. However, the net exchange varies greatly from sub-basin to sub-basin. Kattegat, the western Baltic Sea and the Baltic proper all have annual net uptake of atmospheric CO_2 averaged over 2005 to 2010, while the remaining three sub-basins release CO_2 to the atmosphere. The Baltic proper contributes the most to the total annual averaged flux with an uptake of 254 g C yr^{-1}, but during some individual months the fluxes in the Baltic proper are even larger (up to 900 g C $month^{-1}$). Monthly fluxes of this considerable size are not obtained in any of the other sub-domains. This is of course related to the fact that the Baltic proper has the greatest spatial extent of all the six sub-basins.

To estimate the marine contribution in the Danish national CO_2 budget, the air–sea CO_2 flux in the Danish exclusive economic zone (EEZ) is calculated. The EEZ is a zone adjacent to the territorial waters extending up to 200 nautical miles offshore, and in the EEZ the coastal state has the right to explore, exploit and manage all resources within this area (United Nations Chapter XXI Law of the Sea, 1984). The Danish EEZ has an area of approximately 105 000 km^2 (Fig. S2). During the 6 years simulated, an average annual uptake in the Danish EEZ of 2613 Gg C yr^{-1} is obtained. Here, the annual average of 2616 Gg C yr^{-1} is reported. The interannual variability of the estimated flux will solely be a result of the interannual variations in the atmospheric CO_2, as a climatology is used for the surface water pCO_2^w, due to the limited amount of data. The main part of the uptake in the Danish EEZ occurs in the North Sea. The North Sea has the largest extent in the Danish EEZ and combined with a small seasonal amplitude in pCO_2^w, this results in a constant uptake throughout the year. The other sub-basins within the Danish EEZ all release CO_2 in winter and take up CO_2 during summer. The marine uptake in the Danish EEZ corresponds to 18 % of the yearly Danish national emissions of anthropogenic CO_2 (Table 2). For the 6-year period investigated, the annual mean inventory in CO_2 excluding land use and land use change is 14.6 Tg C (Nielsen et al., 2013).

3.2.2 Constant atmospheric CO_2 concentration

The impact of variations in the atmospheric CO_2 concentration is analysed in the following by comparing the results of the air–sea CO_2 fluxes for the VAT and CAT simulations in the six sub-basins. A total annual difference of 184 Gg C yr^{-1} is obtained, which corresponds to a 64 % difference (calculated with VAT as the reference). CAT gives a total annual uptake of 471 Gg C yr^{-1}, while VAT only has an annual up-

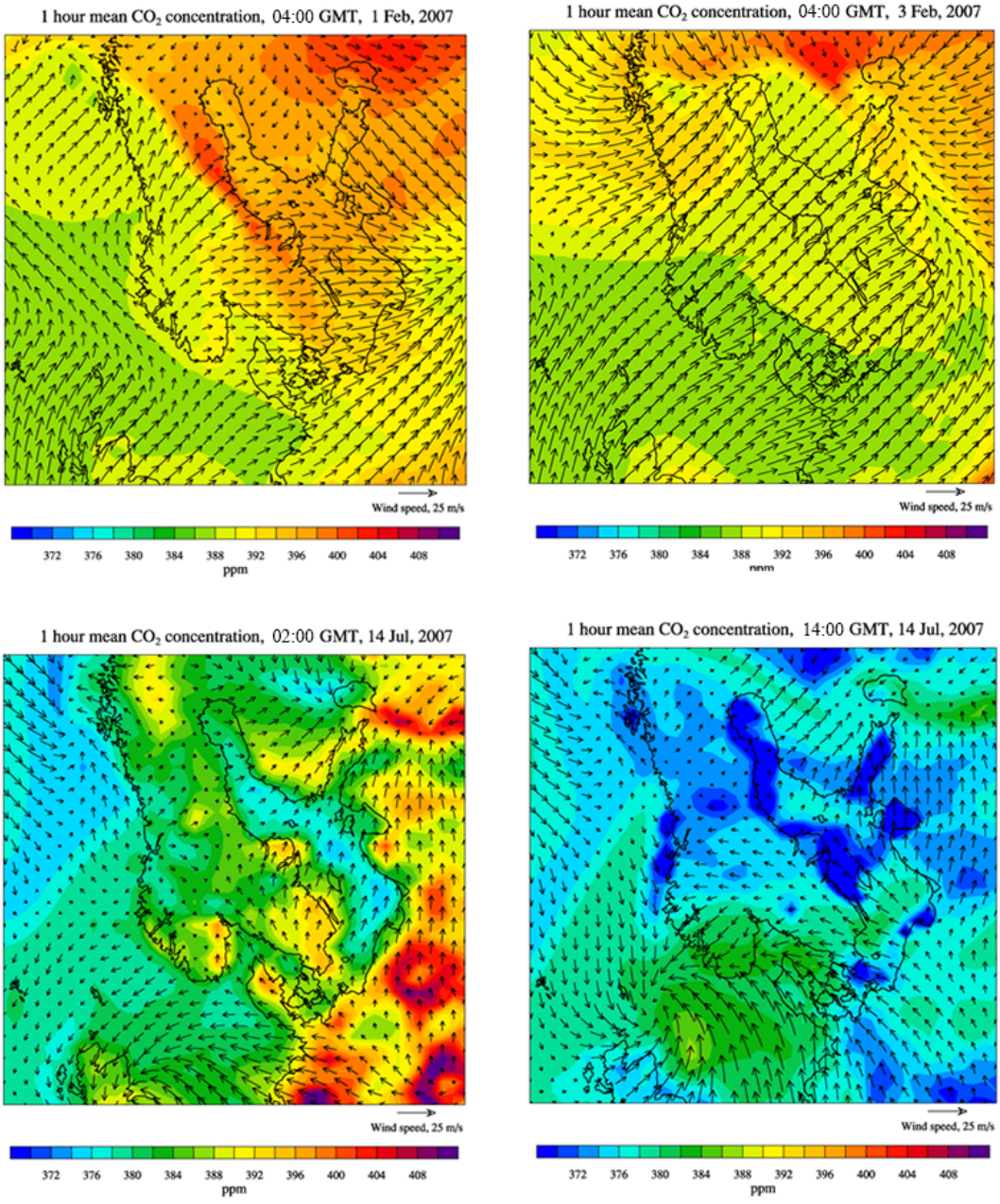

Figure 6. Examples of the simulated variability of atmospheric CO_2 in the study area shown here as extracted from the European domain in DEHM with a 50 km × 50 km resolution. Top panels: two sets of conditions for February 2007. Continental air masses cover the Baltic region on 1 February, while marine air masses are dominating on 3 February. Bottom panels: the diurnal variability on 14 July 2007 (night-time on the left and daytime, right).

take of 287 Gg C yr^{-1}. The seasonal difference between VAT and CAT across the study area is seen in Fig. 8. The monthly fluxes in the sub-basins maintain the same direction in both VAT and CAT. However, for months where the different sub-basins experience outgassing, the outgassing is reduced in the CAT simulation as compared to in the VAT simulation. For months with an uptake of CO_2 in the individual sub-basins, a higher uptake is simulated with the CAT setup than with the VAT setup.

In order to further analyse the difference between the VAT and the CAT simulations, times series of the driving parameters are compared. Examples of the atmospheric pCO_2 (pCO_2^a) in the lowest model layer in the VAT and CAT simulations are shown for a coastal site south of Sweden (55°18′ N, 13°55′ E) in Figs. 9 and 10 for February and July

Table 1. Monthly mean fluxes for the period 2005–2010 in the VAT simulation depicting seasonal variation of the air–sea CO_2 exchange. Values are given in gigagrams of carbon per sub-basin. Positive sign indicates release of CO_2 from the ocean to the atmosphere, negative sign indicates uptake of atmospheric CO_2 by the ocean. This sign convention is used throughout the paper.

	Jan	Feb	Mar	Apr	May	Jun	Jul	Aug	Sep	Oct	Nov	Dec	Ann
Kattegat	29	−21	−98	−42	−25	−28	−26	−33	−33	−15	14	43	**−235**
Western Baltic	125	31	−113	−226	−206	−142	−153	−92	60	137	236	140	**−203**
Baltic proper	804	365	92	−654	−808	−718	−844	−784	−178	481	995	993	**−254**
Gulf of Finland	49	60	8	−61	−92	−68	−74	−67	1	78	151	117	**102**
Bothnian Sea	207	120	83	−253	−383	−325	−355	−284	−22	439	529	412	**167**
Bay of Bothnia	31	23	10	−7	−50	−91	−118	−18	48	205	94	9	**137**

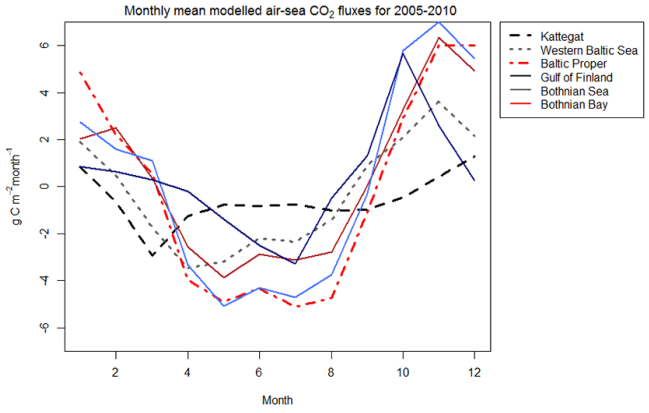

Figure 7. The monthly mean air–sea CO_2 flux for the years 2005 to 2010 in the six sub-basins in $g\,C\,m^{-2}\,month^{-1}$ for the VAT simulation.

2007, respectively. This site is chosen as it can be influenced by air masses from both land and sea depending on the wind direction.

February represents a case of outgassing, and July a case of marine uptake of atmospheric CO_2. Time series of wind velocity at 10 m, u_{10}, and the atmospheric mixing height, h_{mix}, are also plotted to get indications of horizontal transport and vertical mixing. In addition, the differences in the atmospheric partial pressure of CO_2 (ΔpCO_2^a) and in the air–sea CO_2 flux (ΔF_{CO_2}) between the two simulations are shown (calculated as VAT – CAT). Differences in the pCO_2^a in the two simulations determine the difference in pCO_2 between the two simulations as the partial pressure of CO_2 in the water is the same in the two simulations. pCO_2^a is the only variable allowed to vary in the air–sea CO_2 flux calculations between VAT and CAT, and is thus responsible for the obtained flux difference.

For both months, pCO_2^a_VAT fluctuates around the constant pCO_2^a_CAT. During the first half of February, a period of anti-correlation between pCO_2^a_VAT and u_{10} is seen. This anti-correlation is greatest during the second week with a weekly correlation coefficient (r) equal to −0.69. Thus, for this period the episodes of high wind speed tend to dilute the pCO_2^a levels allowing for a greater ΔpCO_2 in the VAT simulation than in the CAT simulation. During the last week of February, a positive correlation of $r = 0.62$ between the two parameters is obtained with wind speeds above $10\,m\,s^{-1}$ and high pCO_2^a levels in the atmosphere. This gives smaller ΔpCO_2 in the VAT simulation than in the CAT simulation, which results in greater fluxes in the CAT simulation. In February, no clear diurnal cycle is seen in the mixing height, but the mixing height seems to follow the pattern of the wind speed with decreases in h_{mix} during periods with low wind speeds and increases in h_{mix} during high wind speeds. The correlation between these two parameters in February is $r = 0.72$. Hence, in February the pCO_2^a_VAT levels are dominated by horizontal transport.

In July, a clear diurnal variability is seen in pCO_2^a_VAT, and an anti-correlation between h_{mix} and pCO_2^a_VAT is evident throughout the month with the highest anti-correlation during the last week (with $r = -0.72$). During July, the so-called diurnal rectifier effect is modelled by the VAT simulation. The rectifier effect is most apparent during the growing season and can be described as the collaboration between terrestrial ecosystems and boundary layer dynamics that act towards lowering pCO_2^a during the day and increase it during night (Denning et al., 1996). Due to the constant level of atmospheric CO_2 in the CAT simulation, the rectifier effect is absent here. This results in a greater uptake of atmospheric CO_2 in the CAT simulation than the VAT simulation during the growing season.

An anti-correlation between ΔpCO_2^a and ΔF_{CO_2} is seen in both February and July. During winter, the largest difference in the air–sea CO_2 flux between VAT and CAT coincides with high wind speeds or large differences in the atmospheric CO_2 concentrations (hence large ΔpCO_2^a values). In summer, the diurnal cycle in the atmospheric CO_2 levels are translated into the flux difference.

Vertical profiles of atmospheric CO_2 at the site south of Sweden have been plotted together with h_{mix} in Fig. 11. Note that the unit in Fig. 11 is parts per million and not microatmosphere. The variability of CO_2 is also evident in the vertical profile, where air masses with low or high CO_2 concentrations are being transported to and from the site (55°18′ N,

Table 2. Annual Danish CO_2 emissions as reported to UNFCCC. The middle row contains the annual uptake of CO_2 in the marine area defined as the Danish exclusive economic zone as estimated in this study. The bottom rows give this uptake as a percentage of the Danish anthropogenic CO_2 emissions.

	2005	2006	2007	2008	2009	2010	6 yr average
CO_2 (Tg C)	14.3	16.5	15.2	14.3	13.6	13.7	**14.6**
Total uptake EEZ (Tg C)	−2.6	−2.4	−2.8	−2.6	−2.6	−2.7	**-2.6**
% of CO_2	18	14	18	18	19	20	**18**

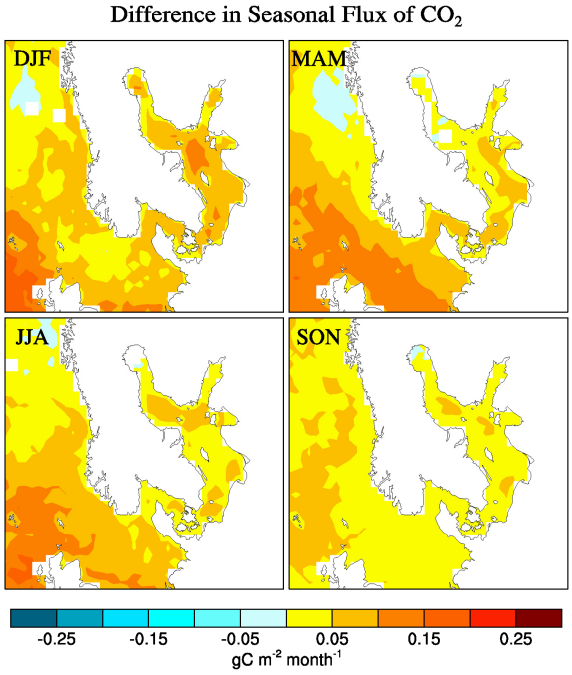

Figure 8. The seasonal flux difference between the VAT and CAT simulations for the period 2005 to 2010 in g C m^{-2} $month^{-1}$ calculated as VAT−CAT. In winter, the fluxes in both VAT and CAT are positive, but larger in VAT than CAT, and thus the difference is positive. In summer, both the fluxes in VAT and CAT are negative, but CAT is numerical larger than VAT, and thus the difference is also positive.

13°55′ E). Continental air is represented by high levels of CO_2 that extend up to 2 km into the atmosphere, while marine air masses have lower levels of CO_2 corresponding to the levels above 2 km. The shift between the two types of air masses is clearly seen in the vertical profile; e.g on 2 February. Here, higher wind speed leads to transport of marine air masses to the site (see Fig. 9). Like Fig. 9, the vertical profile in February shows no clear connection between surface concentrations of CO_2 and h_{mix}. In July, the vertical profile depicts the rectifier effect. Low surface values of CO_2 coincide with the greatest boundary layer heights found during the daytime, and high surface levels of CO_2 concur during nighttime with the nocturnal boundary layer. It is remarkable how the vertical profile during July 2007 represents a much more mixed atmosphere as compared to February 2007, where the marine and continental air masses clearly are distinguished from each other.

4 Discussion

4.1 Surface water pCO_2^w climatology

A representative map of surface pCO_2^w has been created for Skagerrak and six sub-domains in the Baltic using two data sets: one obtained from monitoring stations and one using on-board measurements of surface pCO_2^w (see Sect. 2.2).

Previous estimates of pCO_2^w at two positions within the Baltic Sea have shown interannual variability of up to 25 % in winter and almost 140 % in summer (Wesslander et al., 2010). Likewise, large short-term variability has been measured in different coastal systems (Dai et al., 2009; Leinweber et al., 2009; Wesslander et al., 2011).

The representation of surface pCO_2^w values in the subdomains by a monthly averaged value does not account for the temporal variability during each month and the spatial variability in the relatively large areas. The estimated surface fields of pCO_2^w are based on all available data; however, the amount of available observations can be considered to be relatively small compared to the large study area, although on-board pCO_2^w measurements (Schneider and Sadkowiak, 2012) have increased the data coverage in the central Baltic Sea significantly in the past few years.

The choice of applying a surface map of pCO_2^w for six domains in the Baltic of course introduces some biases on the flux estimates as mechanisms, such as upwelling and algae blooms that act on a smaller spatial scale than the subdivision, are not specifically accounted for. It was essential for the present study to obtain a surface map of pCO_2^w that covered the entire region to be able to study the effect of short-term variability in atmospheric CO_2 on the air–sea CO_2 flux within the Baltic Sea region. Despite the possible biases of ignoring short-term and small-scale variability in ocean pCO_2^w, the simplified description of the conditions in the Baltic Sea in a number of sub-domains was evaluated to be the best solution to obtain a surface field of pCO_2^w that spatially covers the whole model domain for the present study.

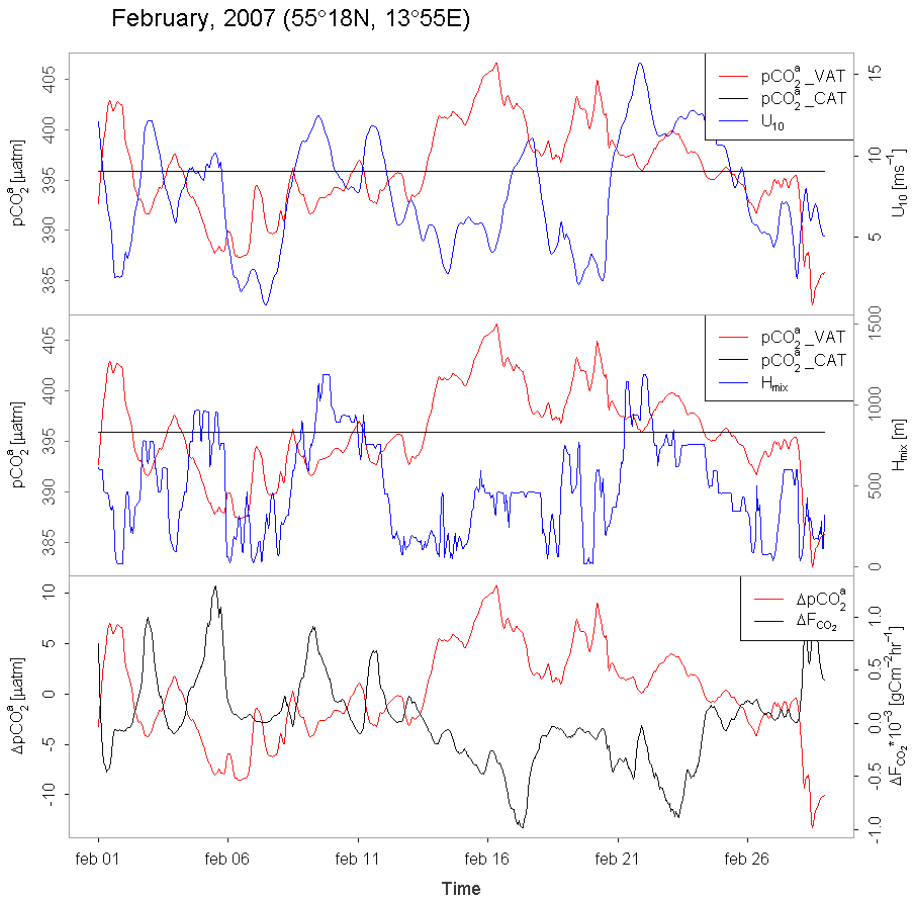

Figure 9. Time series of driving parameters as extracted from the simulations at the site south of Sweden (55°18′ N, 13°55′ E) in February 2007. Top panel: pCO_2^a for VAT and CAT together with u_{10}. Middle panel: pCO_2^a for VAT and CAT together with h_{mix}. Bottom panel: difference in pCO_2^a (ΔpCO_2^a) and F_{CO_2} (ΔF_{CO_2}) between VAT and CAT.

4.2 Air–sea CO_2 fluxes

The atmospheric CO_2 concentration is seen to vary greatly within the study area (Figs. 6 and 11). The dynamics of the fluxes and the atmospheric transport and mixing lead to short-term variations and spatial gradients in the atmospheric CO_2 level across the study area. Pressure systems move through the region transporting air masses with different characteristics and CO_2 levels to and from the Baltic and the Danish inner waters. In the growing season, the effect from the terrestrial biosphere is apparent, with a clear diurnal cycle in the atmospheric CO_2 caused by respiration during night-time and photosynthesis during the day, complemented by boundary layer dynamics. Even these short-term variations in atmospheric CO_2 concentrations over land can be transported to marine areas, indicating why it is important to include atmospheric short-term variability in the air–sea flux estimations.

For the 6-year period, an annual average uptake of 287 Gg C yr^{-1} is obtained with the VAT setup as a total for the six sub-basins. A statistical analysis of the simulated fluxes shows that Kattegat and the western Baltic Sea are annual sinks (at a significance level of 0.05), while the Gulf of Finland and the Bay of Bothnia are annual sources of atmospheric CO_2. In the transition zone between these areas, i.e. the Baltic proper and the Bothnian Sea, large variations in the annual flux are seen in this study. During the 6 years simulated, these sub-domains change annually between being sources and sinks of CO_2 to the atmosphere. This also affects the total flux for the entire investigated area, which also shifts between being an annual source (376 Gg C yr^{-1}) and sink (−1100 Gg C yr^{-1}). A significant test (Student's t test with a significance level of 0.05) show that the variability from year to year during the 6 years simulated is so large that we cannot conclude that the area is a net sink, despite the estimated averaged uptake of 287 Gg C yr^{-1}.

The air–sea CO_2 fluxes obtained from the VAT simulation for six sub-basins are compared to previous results from the area to assess consistency. Previous studies of the air–sea CO_2 flux in the Baltic Sea area are ambiguous on the Baltic Sea's role in the carbon cycle (see Table 3). This is partly caused by the various techniques used, ranging from

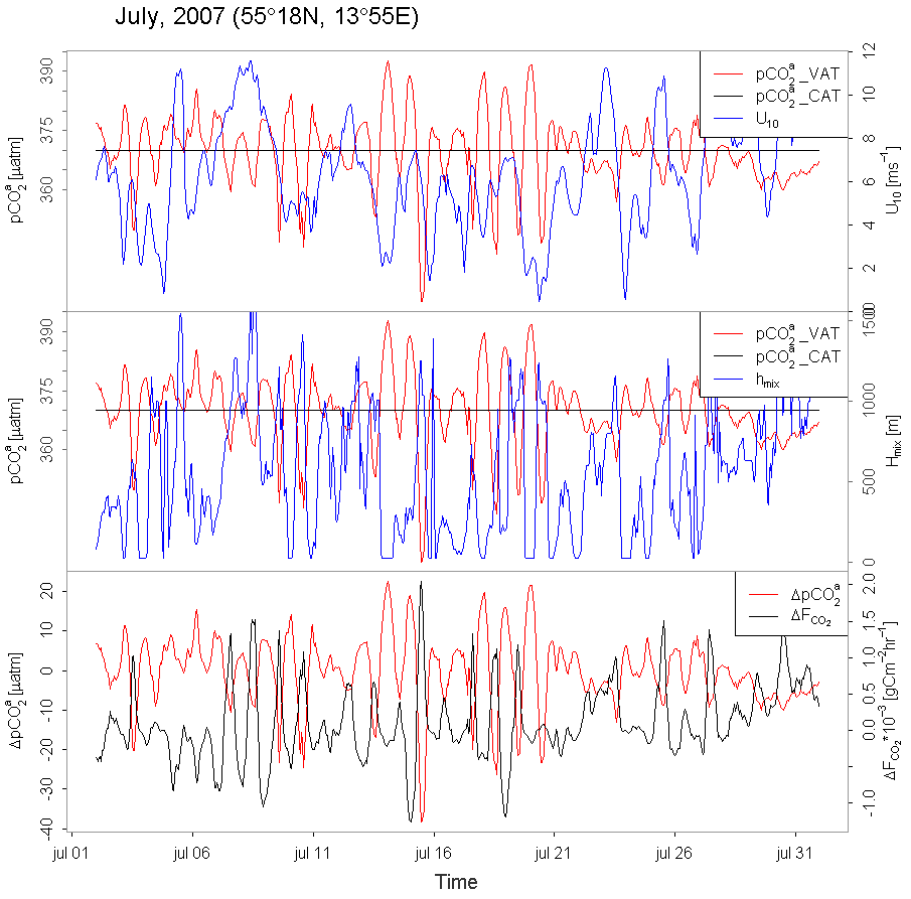

Figure 10. Simulated parameters as in Fig. 9 at the site south of Sweden (55°18′ N, 13°55′ E), but for July, 2007. Top panel: pCO_2^a for VAT and CAT together with u_{10}. Middle panel: pCO_2^a for VAT and CAT together with h_{mix}. Bottom panel: difference in pCO_2^a (ΔpCO_2^a) and F_{CO_2} (ΔF_{CO_2}) between VAT and CAT.

in situ measurements using the eddy covariance method to model simulations (Kulinski and Pempkowiak, 2011; Rutgersson et al., 2009; Weiss et al., 2007; Wesslander et al., 2010), and partly by the different spatial areas investigated. Some of the previous studies are site specific (Algesten et al., 2006; Kuss et al., 2006; Löffler et al., 2012; Rutgersson et al., 2008; Wesslander et al., 2010) and other studies cover the entire area (Gustafsson et al., 2014; Kulinski and Pempkowiak, 2011; Norman et al., 2013). None of the previous regional studies have based their estimates of the air–sea CO_2 flux on results from an atmospheric transport model capable of combining large spatial coverage with high spatiotemporal resolution of the entire Baltic region as in the present study. Results from previous studies and the present study have been converted to the same unit of $g\,C\,m^{-2}\,yr^{-1}$ to allow for a direct comparison (Table 3).

Table 3 reveals that in terms of the direction of the flux, the present study corresponds well with some of the previous studies and contradicts others. As the results obtained from the VAT simulation lie within the range of previous estimates, it seems reasonable to use the current model setup for sensitivity analysis of the air–sea CO_2 flux in the region. Additionally, it can be concluded that the obtained results from the VAT simulation together with recent studies converge towards the Baltic Sea and Danish inner waters being annual sinks of atmospheric CO_2.

4.3 Impact of atmospheric short-term variability

The difference of $184\,Gg\,C\,yr^{-1}$ between the annual air–sea flux in the CAT and VAT simulations was tested to be significantly different from zero at a 0.05 significance level. Therefore, it can be concluded that using a constant level of atmospheric CO_2 has a significant impact on the estimated annual air–sea CO_2 flux in this region. The greatest differences are found in winter and autumn in the Baltic Sea area (Fig. 8). But large differences are also found over open water areas in spite of a less variable atmospheric CO_2 concentration here, i.e. a smaller difference in the atmospheric CO_2 concentration between the two simulations. Despite the small concentration difference, the tendency towards higher wind speeds

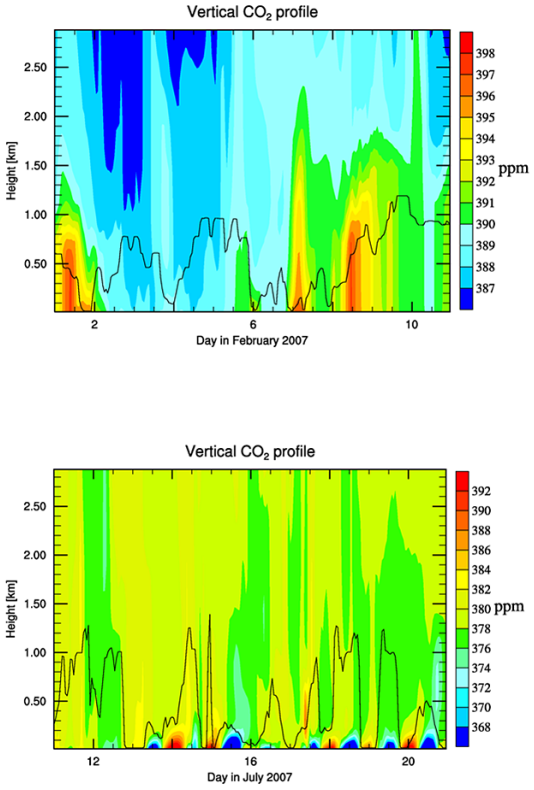

Figure 11. Simulated vertical profiles of atmospheric CO_2 at the site south of Sweden (55°18′ N, 13°55′ E) in units of ppm. Top panel: 1–10 February 2007. Bottom panel: 11–20 July 2007. The black line represents the mixing height in kilometres. Note the different scales used in the two plots.

over open oceans leads to the large flux difference here. The same wind fields are applied in both simulations.

The deviation between the two simulations in the study region is mainly caused by a reduction in the winter uptake in the CAT simulation. The winter outgassing is reduced in CAT, when the pCO_2^a of the CAT is greater than the pCO_2^a of the VAT simulation. Thereby, ΔpCO_2 is smaller in the CAT simulation than the VAT simulation, and the flux will be reduced. Furthermore, the nonlinearity of the wind speed in the parameterisation of the transfer velocity can amplify this reduction, in particular, when high wind speeds coincide with greater ΔpCO_2 in the VAT simulation than in CAT simulation (e.g. as seen in Fig. 9 for the first week of February 2007). This mechanism must have a significant influence, as it results in a greater winter uptake in the VAT simulation then in the CAT simulation.

The higher marine CO_2 uptake in summer by the CAT simulation is a result of diurnal boundary layer dynamics and the diurnal cycle or lack of it in the atmospheric CO_2 concentrations. The rectifier effect is not accounted for in the CAT simulation, and the constant pCO_2^a in CAT is higher during the day and lower during the night than in the VAT simulation. This allows for a greater air–sea ΔpCO_2 in the CAT simulation during day, which together with a tendency of higher wind speeds during daytime increases the oceanic uptake in CAT. This is illustrated by ΔF_{CO_2}, where positive values indicate how the flux is numerical larger in CAT than VAT (see Fig. 10). As described in Sect. 3.1, the diurnal cycle of atmospheric CO_2 is generally underestimated by the DEHM model in near-coastal areas. This could indicate that the difference between the VAT and CAT simulations found during the growing season is a conservative estimate for the fluxes at the near-coastal areas in the Baltic Sea region.

While Rutgersson et al. (2008) found a slightly overestimated seasonal amplitude, when using a constant atmospheric CO_2 concentration, the present study finds that the seasonal cycle of the CAT simulation is displaced downwards as compared to the VAT simulation. This displacement results in a greater annual uptake in the CAT simulation.

4.4 Uncertainties

The estimated air–sea CO_2 flux is controlled by several parameters in the applied model setup: choice of transfer velocity parameterisation, wind speed, temperature, salinity, atmospheric CO_2 concentration and marine pCO_2^w surface values. Each of these is connected with some uncertainty and errors.

Takahashi et al. (2009) estimate the combined precision on the global air–sea flux to be on the order of ±60 % when including a possible climatology bias due to interpolation and under-sampling. The uncertainty might be higher in the current study as the climatology for the pCO_2^w in surface waters used here covers areas where the spatiotemporal variability in the measured pCO_2^w is higher than in open waters. The natural variability within the sub-domains is represented by the standard deviations in Fig. 2, and it reflects both the spatial and temporal variation in the domains during the period of sampling, i.e. the last decade. The Baltic Sea domains (i.e. excepting the Kattegat sub-domain) are all characterised by a significant under-saturation of the surface water during spring and summer. During winter, these stations are in general supersaturated with respect to the atmospheric pCO_2^a. Thus, the sign of the CO_2 flux during the seasons is assumed to be well-determined in the Baltic Sea sub-domains due to the large seasonal amplitudes. However, during the seasonal change between summer and winter, where typical standard deviations in the climatology of 50 ppm are seen, we estimate that the uncertainty due to the ocean surface pCO_2^w values is on the order of 50 % in the Baltic Sea. The uncertainty in the Kattegat sub-domain is estimated to be up to 50–100 % because of the relatively small seasonal amplitude.

Atmospheric CO_2, wind speed and temperature all vary in each model time step and grid cell. The uncertainties of wind speed and temperature are small compared to the uncertainties of the pCO_2^w fields. Figures 4 and 5 show how well the DEHM model captures the weekly and seasonal variability in the atmospheric CO_2 concentrations. However, some prob-

Table 3. Present study compared to previous results within the different sub-domains. Study type indicates the type of previous study (Mod. – model based, MBA – mass balance approach, Meas. – measurement based, Cru. – cruise based) and its spatial extent (sb – sub-basins, ss – site specific). All shown results are in $g\,C\,m^{-2}\,yr^{-1}$.

	Previous results	Study	Study type	Present Study
Kattegat	−40.0	Gustafsson et al. (2014)	Mod., sb	−7.0
	19.0	Norman et al. (2013)	Mod., sb	
	−13.9	Wesslander et al. (2010)	Meas., ss	
Western Baltic	−34	Gustafsson et al. (2014)	Mod., sb	−3.1
	−36.0	Kuss et al. (2006)	Meas., ss	
	−14.4 to 17.9	Norman et al. (2013)	Mod., sb	
	28.1	Wesslander et al. (2010)	Meas., ss	
Baltic proper	−4.2 to −4.3	Norman et al. (2013)	Mod., sb	−1.5
	−10.8	Schneider and Thomas (1999)	Cru., sb	
	19.7	Wesslander et al. (2010)	Meas., ss	
Bothnian Sea	2.2	Gustafsson et al. (2014)	Mod., sb	2.2
	−8.8	Löffler et al. (2012)	Cru., sb	
	−0.6	Norman et al. (2013)	Mod., sb	
Bay of Bothnia	12.0	Gustafsson et al. (2014)	Mod., sb	3.8
	1.7	Löffler et al. (2012)	Cru., sb	
	4.3	Norman et al. (2013)	Mod., sb	
Gulf of Finland	7.4	Norman et al. (2013)	Mod., sb	4.3
Total Baltic Sea	2.7	Kulinski and Pempkowiak (2010)	MBA, sb	−0.7
	−4.3	Gustafsson et al. (2014)	Mod., sb	
	−2.6	Norman et al. (2013)	Mod., sb	

lems arise in capturing the variability on shorter timescales (e.g. diurnal). The diurnal cycle is under-estimated in this model setup, which is related to the coarse resolution of the biosphere fluxes, and of the model itself.

Short-term variability does not only exist in the atmospheric concentration of CO_2, it has also been detected in the pCO_2^w of surface water (Dai et al., 2009; Leinweber et al., 2009; Rutgersson et al., 2008; Wesslander et al., 2011). The magnitude of the short-term variability is site dependent with the smallest variability found in open oceans (Dai et al., 2009) and greatest at near-coastal sites (Leinweber et al., 2009; Wesslander et al., 2011). Off the Californian coast, Leinweber et al. (2009) found a diurnal cycle of pCO_2^w with an average amplitude of 20 µatm – a diurnal amplitude double of what they found in the atmosphere. Short-term variability of marine pCO_2^w, could potentially alter the annual estimate of the coastal air–sea CO_2 flux. Thus, in the present study the fluxes at the near-coastal areas within the sub-domain could be affected by this short-term variability, and as a result possibly modify the total flux for these sub-domains. However, the short-term variability in marine pCO_2^w is not included in this study, and it is, therefore, difficult to estimate how this might affect the estimated flux. Additionally, the short-term variability in the air and water might be correlated, thus it is not possible to make a deduction of the combined effect in the present model study.

To assess the uncertainty connected to the choice of transfer velocity on the estimated air–sea flux model, simulations using parameterisations of Nightingale et al. (2000) and Weiss et al. (2007) have also been conducted. Throughout the seasons, the parameterisation by Weiss et al. (2007) gives more extreme values than that of Nightingale et al. (2000), but the annual sum for the study area results in −667 and $-858\,Gg\,C\,yr^{-1}$ for Nightingale et al. (2000) and Weiss et al. (2007), respectively. Other transfer velocity parameterisations could also have been interesting to use in the present study. An example is the parameterisation by Sweeney et al. (2007), which is based on an updated and improved version of the radiocarbon method used in W92. Here, the two different parameterisations by Weiss et al. (2007) and Nightingale et al. (2000) were chosen, as these experiments were conducted within and close to the study area, respectively.

The present study supports the findings briefly touched upon by Rutgersson et al. (2009), who concluded that the uncertainty due to the value of atmospheric CO_2 is small compared to uncertainty in transfer velocity. Introducing a surface pCO_2^w climatology in six sub-basins adds substantially to the uncertainty, as short-term variability in both space and time is ignored in this parameter. However, we have chosen to use this surface pCO_2^w climatology to get full spatial and temporal coverage of surface pCO_2^w. This allows us to inves-

tigate the effect of short-term variability in atmospheric CO_2 concentration on the air–sea CO_2 flux.

5 Conclusions

Using an atmospheric CO_2 model with a relative high spatial and temporal resolution, we have estimated the air–sea flux of CO_2 in the Danish inner waters and the Baltic Sea region. More specifically we have made a detailed analysis of the sensitivity to temporal variability in atmospheric CO_2 and the related impact of driving parameters like wind speed and atmospheric mixing height.

In the process of this study new monthly marine pCO_2^w fields have been developed for the region combining existing data from monitoring stations and measurements from ships. Due to the sparseness of these data, only seasonal variations are included in the pCO_2^w fields.

The atmospheric concentration of CO_2 is often assumed to be constant or only vary by season in many marine model studies, but according to this novel sensitivity analysis, neglecting, for example, the diurnal and synoptic variability in atmospheric CO_2 concentrations could lead to a systematic bias in the annual net air–sea flux. Previous studies have looked at the entire Baltic region (Gustafsson et al., 2014; Kulinski and Pempkowiak, 2011; Norman et al., 2013; Thomas and Schneider, 1999), but not with the same approach as in the present study.

In all the included sub-basins, a seasonal cycle was detected in the air–sea CO_2 flux with release of CO_2 during winter and autumn, and uptake of atmospheric CO_2 in the remaining months. An annual flux for the study area of $-287\,\mathrm{Gg\,C\,yr^{-1}}$ ($-0.7\,\mathrm{g\,C\,m^{-2}\,yr^{-1}}$) was obtained for the 6 years simulated. This agrees with the previous findings of Norman et al. (2013) and Gustafsson et al. (2014), who estimated annual air–sea CO_2 fluxes of -2.6 and $-4.3\,\mathrm{g\,C\,m^{-2}\,yr^{-1}}$, respectively.

The importance of short-term variations in the atmospheric CO_2 in relation to the yearly air–sea flux was tested with two different model simulations. One simulation includes the short-term variations (the VAT simulation), while the other simulation includes a monthly constant atmospheric CO_2 concentration (the CAT simulation). A significant difference of $184\,\mathrm{Gg\,C\,yr^{-1}}$ (corresponding to 67 %) was obtained for the air–sea CO_2 flux for the Baltic Sea and Danish inner waters between the two model simulations. The seasonal amplitude of the air–sea CO_2 flux was shifted downwards in the CAT simulation as compared to the VAT simulation, resulting in a reduced winter release of CO_2 in the CAT simulation and an increased summer uptake. The difference occurs solely due to the difference in the atmospheric CO_2 concentrations.

As a part of the Danish project ECOCLIM with a focus on the Danish CO_2 budget, the natural marine annual flux of CO_2 was estimated for the first time in the present study. The Danish waters – in this context defined as the Danish exclusive economic zone – is according to our simulations taking up $2613\,\mathrm{Gg\,C\,yr^{-1}}$ with the majority taken up in the North Sea. This is comparable to approximately 18 % of the Danish anthropogenic CO_2 emissions.

Uncertainties are bound to the results, particularly in connection with transfer velocity parameterisation and the applied surface pCO_2^w climatology. However, in the present study, with two model simulations that only differ in atmospheric CO_2 concentrations, a distinguishable difference in the air–sea CO_2 flux is obtained. This, therefore, stresses the importance of including short-term variability in the atmospheric CO_2 in order to minimise the uncertainties in the air–sea CO_2 flux. Moreover, this deduce that also short-term variability in pCO_2^w of the water, in particular of coastal areas, needs to be included, as short-term variability in near-coastal surface water pCO_2^w potentially is greater than in the atmosphere.

To conclude, we recommend that future studies of the air–sea CO_2 exchange include short-term variability of CO_2 in the atmosphere. Thereby, the uncertainty related to estimating the marine part of the carbon budget at regional to global scales can be reduced.

The Supplement related to this article is available online at doi:10.5194/bg-12-2753-2015-supplement.

Acknowledgements. This study is a part of a PhD project within ECOCLIM funded by the Danish Strategic Research Council (grant no. 10-093901). Further, several scientists involved with this work are likewise connected to the Nordic Centre of Excellence, DEFROST. We are grateful to Anna Rutgersson at Uppsala University for sharing atmospheric measurements of CO_2 at Östergarnsholm. We likewise thank the community for making observations available at Lutjewad, Mace Head, Pallas-Sammaltunturi and Westerland. We thank the Swedish Meteorological and Hydrological Institute for sharing marine data from the six monitoring sites. Results from CarbonTracker CT2011_oi provided by NOAA ESRL, Boulder, Colorado, USA from the website at http://carbontracker.noaa.gov contributed to this work, as have GLOBALVIEW-CO2, 2013 and European and Danish fossil fuel emission inventories from IER and Aarhus University, respectively. We are grateful for the very constructive comments from the two anonymous reviewers.

Edited by: S. M. Noe

References

Algesten, G., Brydsten, L., Jonsson, P., Kortelainen, P., Löfgren, S., Rahm, L., Räike, A., Sobek, S., Tranvik, L., Wikner, J., and Jansson, M.: Organic carbon budget for the Gulf of Bothnia, J. Marine Syst., 63, 155–161, 2006.

Bendtsen, J., Gustafsson, K. E., Söderkvist, J., and Hansen, J. L. S.: Ventilation of bottom water in the North Sea-Baltic Sea transition zone, J. Marine Syst., 75, 138–149, 2009.

Biraud, S., Ciais, P., Ramonet, M., Simmonds, P., Kazan, V., Monfray, P., O'Doherty, S., Spain, T. G., and Jennings, S. G.: European greenhouse gas emissions estimated from continuous atmospheric measurements and radon 222 at Mace Head, Ireland, J. Geophys. Res.-Atmos, 105, 1351–1366, 2000.

Boden, T. A., Marland, G., and Andres, R. J.: Global, Regional, and National Fossil-Fuel CO_2 Emissions, Carbon Dioxide Information Analysis Center, Oak Ridge National Laboratory, U. S. Department of Energy, Oak Ridge, Tenn., USA, doi:10.3334/CDIAC/00001_V2013, 2013.

Borges, A. V., Schiettecatte, L. S., Abril, G., Delille, B., and Gazeau, E.: Carbon dioxide in European coastal waters, Estuar. Coast. Shelf S., 70, 375–387, 2006.

Boyer, T., Levitus, S., Garcia, H., Locarnini, R. A., Stephens, C., and Antonov, J.: Objective analyses of annual, seasonal, and monthly temperature and salinity for the world ocean on a 0.25 degrees grid, Int. J. Climatol., 25, 931–945, 2005.

Brandt, J., Silver, J. D., Frohn, L. M., Geels, C., Gross, A., Hansen, A. B., Hansen, K. M., Hedegaard, G. B., Skjøth, C. A., Villadsen, H., Zare, A., and Christensen, J. H.: An integrated model study for Europe and North America using the Danish Eulerian Hemispheric Model with focus on intercontinental transport of air pollution, Atmos. Environ., 53, 156–176, 2012.

Cai, W. J.: Estuarine and Coastal Ocean Carbon Paradox: CO_2 Sinks or Sites of Terrestrial Carbon Incineration?, Annu. Rev. Mar. Sci., 123—145, 2011.

CarbonTracker CT2011_oi, http://carbontracker.noaa.gov, last access: 1 August 2013.

Chen, C. T. A. and Borges, A. V.: Reconciling opposing views on carbon cycling in the coastal ocean: Continental shelves as sinks and near-shore ecosystems as sources of atmospheric CO_2, Deep-Sea Res. Pt. II, 56, 578–590, 2009.

Chen, C.-T. A., Huang, T.-H., Chen, Y.-C., Bai, Y., He, X., and Kang, Y.: Air-sea exchanges of CO_2 in the world's coastal seas, Biogeosciences, 10, 6509–6544, doi:10.5194/bg-10-6509-2013, 2013.

Christensen, J. H.: The Danish Eulerian hemispheric model – A three-dimensional air pollution model used for the Arctic, Atmos. Environ., 31, 4169–4191, 1997.

Dai, M. H., Lu, Z. M., Zhai, W. D., Chen, B. S., Cao, Z. M., Zhou, K. B., Cai, W. J., and Chen, C. T. A.: Diurnal variations of surface seawater pCO_2 in contrasting coastal environments, Limnol. Oceanogr., 54, 735–745, 2009.

Denning, A. S., Randall, D. A., Collatz, G. J., and Sellers, P. J.: Simulations of terrestrial carbon metabolism and atmospheric CO_2 in a general circulation model 2 Simulated CO_2 concentrations, Tellus B, 48, 543–567, 1996.

FMI: Atmospheric CO_2 hourly concentration data, Pallas-Sammaltunturi – FMI, WMO World Data Centre for Greenhouse Gases, Japan Meteorol. Agency, Tokyo, 2013.

Garbe, C. S., Rutgersson, A., Boutin, J., de Leeuw, G., Delille, B., Fairall, C. W., Gruber, N., Hare, J., Ho, D. H., Johnson, M. T., Nightingale, P. D., Pettersson, H., Piskozub, J., Sahlee, E., Tsai, W., Ward, B., Woolf, D. K., and Zappa, C. J.: Transfer Across the Air-Sea Interface, in: Ocean-Atmosphere Interactions of Gases and Particles, edited by: Liss, P. S. and Johnson, M. T., Springer, Earth System Science, 55–111, 2014.

Gattuso, J. P., Frankignoulle, M., and Wollast, R.: Carbon and carbonate metabolism in coastal aquatic ecosystems, Annu. Rev. Ecol. Syst., 29, 405–434, 1998.

Geels, C., Christensen, J. H., Frohn, L. M., and Brandt, J.: Simulating spatiotemporal variations of atmospheric CO_2 using a nested hemispheric model, Phys. Chem. Earth., 27, 1495–1505, 2002.

Geels, C., Doney, S. C., Dargaville, R., Brandt, J., and Christensen, J. H.: Investigating the sources of synoptic variability in atmospheric CO_2 measurements over the Northern Hemisphere continents: a regional model study, Tellus B, 56, 35–50, 2004.

Geels, C., Gloor, M., Ciais, P., Bousquet, P., Peylin, P., Vermeulen, A. T., Dargaville, R., Aalto, T., Brandt, J., Christensen, J. H., Frohn, L. M., Haszpra, L., Karstens, U., Rödenbeck, C., Ramonet, M., Carboni, G., and Santaguida, R.: Comparing atmospheric transport models for future regional inversions over Europe – Part 1: mapping the atmospheric CO_2 signals, Atmos. Chem. Phys., 7, 3461–3479, doi:10.5194/acp-7-3461-2007, 2007.

Geels, C., Hansen, K. M., Christensen, J. H., Ambelas Skjøth, C., Ellermann, T., Hedegaard, G. B., Hertel, O., Frohn, L. M., Gross, A., and Brandt, J.: Projected change in atmospheric nitrogen deposition to the Baltic Sea towards 2020, Atmos. Chem. Phys., 12, 2615–2629, doi:10.5194/acp-12-2615-2012, 2012.

Giglio, L., van der Werf, G. R., Randerson, J. T., Collatz, G. J., and Kasibhatla, P.: Global estimation of burned area using MODIS active fire observations, Atmos. Chem. Phys., 6, 957–974, doi:10.5194/acp-6-957-2006, 2006.

GLOBALVIEW-CO2: Cooperative Global Atmospheric Data Integration Project, 2013, updated annually, Multi-laboratory compilation of synchronized and gap-filled atmospheric carbon dioxide records for the period 1979–2012 (obspack_co2_1_GLOBALVIEW-CO2_2013_v1.0.4_2013-12-23), Compiled by NOAA Global Monitoring Division: Boulder, Colorado, USA, doi:10.3334/OBSPACK/1002, 2013.

Grell, G. A., Dudhia, J., and Stauffer, D. R.: A Description of the Fifth-generation Penn State/NCAR Mesoscale Model (MM5), National Center for Atmospheric Research, Boulder, Colorado, USA, NCAR Technical Note NCAR/TN-398+STR, 122 pp., 1995.

Gustafsson, E., Deutsch, B., Gustafsson, B. G., Humborg, C., and Mörth, C. M.: Carbon cycling in the Baltic Sea - The fate of allochthonous organic carbon and its impact on air-sea CO_2 exchange, J. Marine Syst., 129, 289–302, 2014.

Högström, U., Sahlée, E., Drennan, W. M., Kahma, K. K., Smedman, A. S., Johansson, C., Pettersson, H., Rutgersson, A., Tuomi, L., Zhang, F., and Johansson, M.: Momentum fluxes and wind gradients in the marine boundary layer – a multi-platform study, Boreal Environ. Res., 13, 475–502, 2008.

Körtzinger, A., Thomas, H., Schneider, B., Gronau, N., Mintrop, L., and Durr, H. H.: At sea intercompariosn of two newly designed underway pCO_2 systems – encouraging results, Mar. Chem., 52, 133–145, 1996.

Kuliński, K. and Pempkowiak, J.: The carbon budget of the Baltic Sea, Biogeosciences, 8, 3219–3230, doi:10.5194/bg-8-3219-2011, 2011.

Kuss, J., Roeder, W., Wlost, K. P., and DeGrandpre, M. D.: Time-series of surface water CO_2 and oxygen measurements on a plat-

form in the central Arkona Sea (Baltic Sea): Seasonality of uptake and release, Mar. Chem., 101, 220–232, 2006.

Langner, J., Andersson, C., and Engardt, M.: Atmospheric input of nitrogen to the Baltic Sea basin: present situation, variability due to meteorology and impact of climate change, Boreal Environ. Res., 14, 226–237, 2009.

Laruelle, G. G., Durr, H. H., Slomp, C. P., and Borges, A. V.: Evaluation of sinks and sources of CO_2 in the global coastal ocean using a spatially-explicit typology of estuaries and continental shelves, Geophys. Res. Lett., 37, L15607, 2010.

Leinweber, A., Gruber, N., Frenzel, H., Friederich, G. E., and Chavez, F. P.: Diurnal carbon cycling in the surface ocean and lower atmosphere of Santa Monica Bay, California, Geophys. Res. Lett., 36, L08601, 2009.

Le Quéré, C., Andres, R. J., Boden, T., Conway, T., Houghton, R. A., House, J. I., Marland, G., Peters, G. P., van der Werf, G. R., Ahlström, A., Andrew, R. M., Bopp, L., Canadell, J. G., Ciais, P., Doney, S. C., Enright, C., Friedlingstein, P., Huntingford, C., Jain, A. K., Jourdain, C., Kato, E., Keeling, R. F., Klein Goldewijk, K., Levis, S., Levy, P., Lomas, M., Poulter, B., Raupach, M. R., Schwinger, J., Sitch, S., Stocker, B. D., Viovy, N., Zaehle, S., and Zeng, N.: The global carbon budget 1959–2011, Earth Syst. Sci. Data, 5, 165–185, doi:10.5194/essd-5-165-2013, 2013.

Löffler, A., Schneider, B., Perttila, M., and Rehder, G.: Air-sea CO_2 exchange in the Gulf of Bothnia, Baltic Sea, Cont. Shelf. Res., 37, 46–56, 2012.

Meesters, A. G. C. A., Tolk, L. F., Peters, W., Hutjes, R. W. A., Vellinga, O. S., Elbers, J. A., Vermeulen, A. T., van der Laan, S., Neubert, R. E. M., Meijer, H. A. J., and Dolman, A. J.: Inverse carbon dioxide flux estimates for the Netherlands, J. Geophys. Res.-Atmos, 117, D20306, 2012.

Mørk, E. T., Sørensen, L. L., Jensen, B., and Sejr, M. K.: Air-Sea CO_2 Gas Transfer Velocity in a Shallow Estuary, Bound.-Lay. Meteorol., 151, 119–138, 2014.

Nielsen, O.-K., Plejdrup, M. S., Winther, M., Nielsen, M., Gyldenkærne, S., Mikkelsen, M. H., Albrektsen, R., Thomsen, M., Hjelgaard, K., Hoffmann, L., Fauser, P., Bruun, H. G., Johannsen, V. K., Nord-Larsen, T., Vesterdal, L., Møller, I. S., Caspersen, O. H., Rasmussen, E., Petersen, S. B., Baunbæk, L., and Hansen, M. G.: Denmark's National Inventory Report 2013, Emission Inventories 1990–2011 – Submitted under the United Nations Framework Convention on Climate Change and the Kyoto Protocol, Aarhus University, DCE – Danish Centre for Environment and Energy, 1–1202, 2013.

Nightingale, P. D., Malin, G., Law, C. S., Watson, A. J., Liss, P. S., Liddicoat, M. I., Boutin, J., and Upstill-Goddard, R. C.: In situ evaluation of air-sea gas exchange parameterizations using novel conservative and volatile tracers, Global Biogeochem. Cy., 14, 373–387, 2000.

Norman, M., Rutgersson, A., and Sahlée, E.: Impact of improved air-sea gas transfer velocity on fluxes and water chemistry in a Baltic Sea model, J. Marine Syst., 111, 175–188, 2013.

Omstedt, A., Gustafsson, E., and Wesslander, K.: Modelling the uptake and release of carbon dioxide in the Baltic Sea surface water, Cont. Shelf. Res., 29, 870–885, 2009.

Parmentier, F. J. W., Christensen, T. R., Sørensen, L. L., Rysgaard, S., McGuire, A. D., Miller, P. A., and Walker, D. A.: The impact of lower sea-ice extent on Arctic greenhouse-gas exchange, Nat. Clim. Change, 3, 195–202, 2013.

Peters, W., Jacobson, A. R., Sweeney, C., Andrews, A. E., Conway, T. J., Masarie, K., Miller, J. B., Bruhwiler, L. M. P., Pétron, G., Hirsch, A. I., Worthy, D. E. J., van der Werf, G. R., Randerson, J. T., Wennberg, P. O., Krol, M. C., and Tans, P. P.: An atmospheric perspective on North American carbon dioxide exchange: CarbonTracker, P. Natl. Acad. Sci. USA, 104, 18925–18930, 2007.

Plejdrup, M. S. and Gyldenkærne, S.: Spatial distribution of emissions to air – the SPREAD model, National Environmental Research Institute, Aarhus University, Denmark, 72 pp., 2011.

Pregger, T., Scholz, Y., and Friedrich, R.: Documentation of the Anthropogenic GHG Emission Data for Europe Provided in the Frame of CarboEurope GHG and CarboEurope IP, University of Stuttgart, IER – Institute of Energy Economics and the Rational Use of Energy, 37 pp., 2007.

Rutgersson, A., Norman, M., Schneider, B., Pettersson, H., and Sahlée, E.: The annual cycle of carbon dioxide and parameters influencing the air-sea carbon exchange in the Baltic Proper, J. Marine Syst., 74, 381–394, 2008.

Rutgersson, A., Norman, M., and Åström, G.: Atmospheric CO_2 variation over the Baltic Sea and the impact on air-sea exchange, Boreal Environ. Res., 14, 238–249, 2009.

Sarrat, C., Noilhan, J., Lacarrère, P., Masson, V., Ceschia, E., Ciais, P., Dolman, A., Elbers, J., Gerbig, C., and Jarosz, N.: CO_2 budgeting at the regional scale using a Lagrangian experimental strategy and meso-scale modeling, Biogeosciences, 6, 113–127, doi:10.5194/bg-6-113-2009, 2009.

Schneider, B. and Sadkowiak, B.: Underway pCO_2 Measurements in Surface Waters during the VOS and Research Cruises in Baltic Sea, http://cdiac.ornl.gov/ftp/oceans/Baltic_Sea/, Carbon Dioxide Information Analysis Center, Oak Ridge National Laboratory, US Department of Energy, Oak Ridge, Tennessee, doi:10.3334/CDIAC/OTG.VOS_BALTIC_SEA_LINES, 2012.

Schneider, B., Kaitala, S., and Maunula, P.: Identification and quantification of plankton bloom events in the Baltic Sea by continuous pCO_2 and chlorophyll a measurements on a cargo ship, J. Marine Syst., 59, 238–248, 2006.

SHARK database: SMHI http://www.smhi.se/klimatdata/oceanografi/Havsmiljodata (last acces: 1 May 2014), 2013.

Smallman, T. L., Williams, M., and Moncrieff, J. B.: Can seasonal and interannual variation in landscape CO_2 fluxes be detected by atmospheric observations of CO_2 concentrations made at a tall tower?, Biogeosciences, 11, 735–747, doi:10.5194/bg-11-735-2014, 2014.

Sørensen, L. L., Jensen, B., Glud, R. N., McGinnis, D. F., Sejr, M. K., Sievers, J., Søgaard, D. H., Tison, J.-L., and Rysgaard, S.: Parameterization of atmosphere-surface exchange of CO_2 over sea ice, The Cryosphere, 8, 853–866, doi:10.5194/tc-8-853-2014, 2014.

Sweeney, C., Gloor, E., Jacobson, A. R., Key, R. M., McKinley, G., Sarmiento, J. L., and Wanninkhof, R.: Constraining global air-sea gas exchange for CO2 with recent bomb C-14 measurements, Glob. Biogeochem. Cy., 21, GB2015, doi:10.1029/2006GB002784, 2007.

Takahashi, T., Sutherland, S. C., Wanninkhof, R., Sweeney, C., Feely, R. A., Chipman, D. W., Hales, B., Friederich, G., Chavez, F., Sabine, C., Watson, A., Bakker, D. C. E., Schuster, U., Metzl, N., Yoshikawa-Inoue, H., Ishii, M., Midorikawa, T., Nojiri, Y., Körtzinger, A., Steinhoff, T., Hoppema, M., Olafsson, J., Arnarson, T. S., Tilbrook, B., Johannessen, T., Olsen, A., Bellerby, R.,

Wong, C. S., Delille, B., Bates, N. R., and de Baar, H. J. W.: Climatological mean and decadal change in surface ocean pCO_2, and net sea-air CO_2 flux over the global oceans, Deep-Sea Res. Pt. II, 56, 554–577, 2009.

Thomas, H. and Schneider, B.: The seasonal cycle of carbon dioxide in Baltic Sea surface waters, J. Marine Syst., 22, 53–67, 1999.

Thomas, H., Bozec, Y., Elkalay, K., and de Baar, H. J. W.: Enhanced open ocean storage of CO_2 from shelf sea pumping, Science, 304, 1005–1008, 2004.

UBA: Air Monitoring Network of the Federal Environment Agency (UBA), Germany Monitoring site Westerland, 2014.

United Nations Chapter XXI: Law of the Sea, https://treaties.un.org/Pages/ViewDetailsIII.aspx?&src=TREATY&mtdsg_no=XXI6&chapter=21&Temp=mtdsg3&lang=en (last access: 1 May 2014),1984.

Vainio, J., Eriksson, P., Schmelzer, N., Holfort, J., Grafström, T., Lindberg, A. E. B., Lind, L., Öberg, J., Viksna, A., Križickis, E., Stanisławczyk I., and Sztobryn, M.: The Ice Season 2010–11, HELCOM Baltic Sea Environment Fact Sheets, http://www.helcom.fi/baltic-sea-trends/environment-fact-sheets/ (last access: 23 March 2015), 2011.

van der Laan, S., Neubert, R. E. M., and Meijer, H. A. J.: A single gas chromatograph for accurate atmospheric mixing ratio measurements of CO_2, CH_4, N_2O, SF_6 and CO, Atmos. Meas. Tech., 2, 549–559, doi:10.5194/amt-2-549-2009, 2009.

van der Laan-Luijkx, I. T., Neubert, R. E. M., van der Laan, S., and Meijer, H. A. J.: Continuous measurements of atmospheric oxygen and carbon dioxide on a North Sea gas platform, Atmos. Meas. Tech., 3, 113–125, doi:10.5194/amt-3-113-2010, 2010.

van der Werf, G. R., Randerson, J. T., Giglio, L., Collatz, G. J., Kasibhatla, P. S., and Arellano Jr., A. F.: Interannual variability in global biomass burning emissions from 1997 to 2004, Atmos. Chem. Phys., 6, 3423–3441, doi:10.5194/acp-6-3423-2006, 2006.

Wanninkhof, R.: Relationship Between Wind-Speed and Gas-Exchange Over the Ocean, J. of Geophys. Res-Oceans, 97, 7373–7382, 1992.

Weiss, A., Kuss, J., Peters, G., and Schneider, B.: Evaluating transfer velocity-wind speed relationship using a long-term series of direct eddy correlation CO_2 flux measurements, J. Marine Syst., 66, 130–139, 2007.

Weiss, R. F.: Carbon Dioxide in Water and Seawater: The Solubilty of a Non-ideal Gas, Mar. Chem., 2, 203–215, 1974.

Wesslander, K., Omstedt, A., and Schneider, B.: Inter-annual and seasonal variations in the air-sea CO_2 balance in the central Baltic Sea and the Kattegat, Cont. Shelf. Res., 30, 1511–1521, 2010.

Wesslander, K., Hall, P., Hjalmarsson, S., Lefevre, D., Omstedt, A., Rutgersson, A., Sahlée, E., and Tengberg, A.: Observed carbon dioxide and oxygen dynamics in a Baltic Sea coastal region, J. Marine Syst., 86, 1–9, 2011.